

Appendix E: MCMC priors

Table E.1. Final priors chosen for the one planet model MCMC inference from Sect. 5.1.

Parameter	Unit	GJ 832	GJ 674	Ross 128
K	[m s ⁻¹]	$\mathcal{U}(15, 20)$	$\mathcal{U}(8.2, 9.2)$	$\mathcal{U}(0.5, 5.0)$
P	[d]	$\mathcal{U}(3300, 4300)$	$\mathcal{U}(4.69, 4.70)$	$\mathcal{U}(9.84, 9.88)$ $\mathcal{U}(9.88, 9.92)$
$\sqrt{e} \sin \omega$		$\mathcal{U}(-1, 1)$	$\mathcal{U}(-1, 1)$	$\mathcal{U}(-1, 1)$
$\sqrt{e} \cos \omega$		$\mathcal{U}(-1, 1)$	$\mathcal{U}(-1, 1)$	$\mathcal{U}(-1, 1)$
t_0	[BJD]	$\mathcal{U}(2448500, 2453500)$	$\mathcal{U}(2453160, 2453161)$	$\mathcal{U}(2453577, 2453587)$
ρ	[d]	$\mathcal{U}(1, 500)$	$\mathcal{U}(1, 500)$	$\mathcal{U}(1, 500)$
τ	[d]	$\mathcal{U}(0.1, 200)$	$\mathcal{U}(0.1, 200)$	$\mathcal{U}(0.1, 200)$
$\sigma_{\text{GP},X}$	[d]	$\mathcal{U}(0, 100)$	$\mathcal{U}(0, 100)$	$\mathcal{U}(0, 100)$
s_X	[m s ⁻¹]	$\mathcal{U}(0, 10)$	$\mathcal{U}(0, 10)$	$\mathcal{U}(0, 10)$
μ_X	[m s ⁻¹]	$\mathcal{U}(\overline{RV}_X - 10, \overline{RV}_X + 10)$	$\mathcal{U}(\overline{RV}_X - 10, \overline{RV}_X + 10)$	$\mathcal{U}(\overline{RV}_X - 10, \overline{RV}_X + 10)$

Notes. \overline{RV}_X is the mean value of the RV subset X, where X denotes one of the observation subsets.

Table E.2. Final priors chosen for the two planet model MCMC inference from Sect. 5.1.

Parameter	Unit	Ross 128 b & c
K_1	[m s ⁻¹]	$\mathcal{U}(0.5, 5.0)$
P_1	[d]	$\mathcal{U}(9.84, 9.88)$
$\sqrt{e_1} \sin \omega_1$		$\mathcal{U}(-1, 1)$
$\sqrt{e_1} \cos \omega_1$		$\mathcal{U}(-1, 1)$
$t_{0,1}$	[BJD]	$\mathcal{U}(2453577, 2453587)$
K_2	[m s ⁻¹]	$\mathcal{U}(0.1, 1.0)$
P_2	[d]	$\mathcal{U}(2, 6)$
$\sqrt{e_2} \sin \omega_2$		$\mathcal{U}(-1, 1)$
$\sqrt{e_2} \cos \omega_2$		$\mathcal{U}(-1, 1)$
$t_{0,2}$	[BJD]	$\mathcal{U}(2453579, 2453583)$
ρ	[d]	$\mathcal{U}(1, 500)$
τ	[d]	$\mathcal{U}(0.1, 200)$
$\sigma_{\text{GP},X}$	[d]	$\mathcal{U}(0, 100)$
s_X	[m s ⁻¹]	$\mathcal{U}(0, 10)$
μ_X	[m s ⁻¹]	$\mathcal{U}(\overline{RV}_X - 10, \overline{RV}_X + 10)$

Notes. \overline{RV}_X is the mean value of the RV subset X, where X denotes one of the observation subsets.

Appendix F: Model comparison priors

Table F.1. Combinations of parameters in use for the individual models of the Bayesian model comparison.

	μ_{H-X}	σ_{H-X}	S_0	Q	ω_0	Q_0	f	dQ	P_{GP}	α	Γ	$P_{rot,GP}$
0P	X	X	-	-	-	-	-	-	-	-	-	-
1P _{ecc}	X	X	-	-	-	-	-	-	-	-	-	-
1P _{circ}	X	X	-	-	-	-	-	-	-	-	-	-
2P _{ecc}	X	X	-	-	-	-	-	-	-	-	-	-
2P _{circ}	X	X	-	-	-	-	-	-	-	-	-	-
0P + GP-SHO	X	X	X	X	X	-	-	-	-	-	-	-
0P + GP-dSHO	X	X	-	-	-	X	X	X	X	-	-	-
0P + GP-QP	X	X	-	-	-	-	-	-	-	X	X	X
1P _{ecc} + GP-SHO	X	X	X	X	X	-	-	-	-	-	-	-
1P _{circ} + GP-SHO	X	X	X	X	X	-	-	-	-	-	-	-
1P _{ecc} + GP-dSHO	X	X	-	-	-	X	X	X	X	-	-	-
1P _{circ} + GP-dSHO	X	X	-	-	-	X	X	X	X	-	-	-
1P _{ecc} + GP-QP	X	X	-	-	-	-	-	-	-	X	X	X
1P _{circ} + GP-QP	X	X	-	-	-	-	-	-	-	X	X	X
2P _{ecc} + GP-SHO	X	X	X	X	X	-	-	-	-	-	-	-
2P _{circ} + GP-SHO	X	X	X	X	X	-	-	-	-	-	-	-
2P _{ecc} + GP-dSHO	X	X	-	-	-	X	X	X	X	-	-	-
2P _{circ} + GP-dSHO	X	X	-	-	-	X	X	X	X	-	-	-
2P _{ecc} + GP-QP	X	X	-	-	-	-	-	-	-	X	X	X
2P _{circ} + GP-QP	X	X	-	-	-	-	-	-	-	X	X	X
<hr/>												
	$\sigma_{dSHO,H-X}$	$\sigma_{QP,H-X}$	K_1	P_1	$\sqrt{e_1} \cos \omega_1$	$\sqrt{e_1} \sin \omega_1$	$t_{0,1}$	K_2	P_2	$\sqrt{e_2} \cos \omega_2$	$\sqrt{e_2} \sin \omega_2$	$t_{0,2}$
0P	-	-	-	-	-	-	-	-	-	-	-	-
1P _{ecc}	-	-	X	X	X	X	X	-	-	-	-	-
1P _{circ}	-	-	X	X	X	X	X	-	-	-	-	-
2P _{ecc}	-	-	X	X	X	X	X	X	X	X	X	X
2P _{circ}	-	-	X	X	X	X	X	X	X	X	X	X
0P + GP-SHO	-	-	-	-	-	-	-	-	-	-	-	-
0P + GP-dSHO	X	X	-	-	-	-	-	-	-	-	-	-
0P + GP-QP	-	X	-	-	-	-	-	-	-	-	-	-
1P _{ecc} + GP-SHO	-	-	X	X	X	X	X	-	-	-	-	-
1P _{circ} + GP-SHO	-	-	X	X	X	X	X	-	-	-	-	-
1P _{ecc} + GP-dSHO	X	-	X	X	X	X	X	-	-	-	-	-
1P _{circ} + GP-dSHO	X	-	X	X	X	X	X	-	-	-	-	-
1P _{ecc} + GP-QP	-	X	X	X	X	X	X	-	-	-	-	-
1P _{circ} + GP-QP	-	X	X	X	X	X	X	-	-	-	-	-
2P _{ecc} + GP-SHO	-	-	X	X	X	X	X	X	X	X	X	X
2P _{circ} + GP-SHO	-	-	X	X	X	X	X	X	X	X	X	X
2P _{ecc} + GP-dSHO	X	-	X	X	X	X	X	X	X	X	X	X
2P _{circ} + GP-dSHO	X	-	X	X	X	X	X	X	X	X	X	X
2P _{ecc} + GP-QP	-	X	X	X	X	X	X	X	X	X	X	X
2P _{circ} + GP-QP	-	X	X	X	X	X	X	X	X	X	X	X

Notes. The use of individual seasonal parameters depends on the dataset in question, hence seasons are combined under the placeholder X.

Table F.2. Bayesian priors used during the model comparison.

	GJ 832 HARPS	GJ 674 HARPS	Ross 128 HARPS	Ross 128 RedDots	Ross 128 HARPS+Carnemes
$\mu_{\text{H-pre}}$	$\mathcal{U}(-10, 10)$	$\mathcal{U}(-10, 10)$	$\mathcal{U}(-10, 10)$	–	$\mathcal{U}(-10, 10)$
$\mu_{\text{H-post}}$	$\mathcal{U}(-10, 10)$	$\mathcal{U}(-10, 10)$	$\mathcal{U}(-10, 10)$	–	$\mathcal{U}(-10, 10)$
$\mu_{\text{H-warmup}}$	–	–	–	$\mathcal{U}(-10, 10)$	$\mathcal{U}(-10, 10)$
μ_{carnemes}	–	–	–	–	$\mathcal{U}(-10, 10)$
$\sigma_{\text{H-pre}}$	$\mathcal{U}(0, 30)$	$\mathcal{U}(0, 30)$	$\mathcal{U}(0, 30)$	–	$\mathcal{U}(0, 30)$
$\sigma_{\text{H-post}}$	$\mathcal{U}(0, 30)$	$\mathcal{U}(0, 30)$	$\mathcal{U}(0, 30)$	–	$\mathcal{U}(0, 30)$
$\sigma_{\text{H-warmup}}$	–	–	–	$\mathcal{U}(0, 30)$	$\mathcal{U}(0, 30)$
σ_{carnemes}	–	–	–	$\mathcal{U}(0, 30)$	$\mathcal{U}(0, 30)$
S_0	$\mathcal{U}(0, 200)$	$\mathcal{U}(0, 200)$	$\mathcal{U}(0, 200)$	$\mathcal{U}(0, 200)$	$\mathcal{U}(0, 200)$
Q	$\ln \mathcal{U}(1e-10, 20000.0)$	$\ln \mathcal{U}(1e-10, 20000.0)$	$\ln \mathcal{U}(1e-10, 20000.0)$	$\ln \mathcal{U}(1e-10, 20000.0)$	$\ln \mathcal{U}(1e-10, 20000.0)$
ω_0	$\mathcal{U}(-1, 1)$	$\mathcal{U}(-1, 1)$	$\mathcal{U}(-1, 1)$	$\mathcal{U}(-1, 1)$	$\mathcal{U}(-1, 1)$
Q_0	$\ln \mathcal{U}(0.1, 100000.0)$	$\ln \mathcal{U}(0.1, 100000.0)$	$\ln \mathcal{U}(0.1, 100000.0)$	$\ln \mathcal{U}(0.1, 100000.0)$	$\ln \mathcal{U}(0.1, 100000.0)$
f	$\mathcal{U}(0, 1)$	$\mathcal{U}(0, 1)$	$\mathcal{U}(0, 1)$	$\mathcal{U}(0, 1)$	$\mathcal{U}(0, 1)$
dQ	$\ln \mathcal{U}(0.1, 100000.0)$	$\ln \mathcal{U}(0.1, 100000.0)$	$\ln \mathcal{U}(0.1, 100000.0)$	$\ln \mathcal{U}(0.1, 100000.0)$	$\ln \mathcal{U}(0.1, 100000.0)$
P_{GP}	$\mathcal{U}(1, 200)$	$\mathcal{U}(1, 200)$	$\mathcal{U}(1, 200)$	$\mathcal{U}(1, 200)$	$\mathcal{U}(1, 200)$
α	$\ln \mathcal{U}(1e-10, 1.0)$	$\ln \mathcal{U}(1e-10, 1.0)$	$\ln \mathcal{U}(1e-10, 1.0)$	$\ln \mathcal{U}(1e-10, 1.0)$	$\ln \mathcal{U}(1e-10, 1.0)$
Γ	$\mathcal{U}(0, 10)$	$\mathcal{U}(0, 10)$	$\mathcal{U}(0, 10)$	$\mathcal{U}(0, 10)$	$\mathcal{U}(0, 10)$
$P_{\text{rot,GP}}$	$\mathcal{U}(1, 200)$	$\mathcal{U}(1, 200)$	$\mathcal{U}(1, 200)$	$\mathcal{U}(1, 200)$	$\mathcal{U}(1, 200)$
$\sigma_{\text{dSHO,H-pre}}$	$\mathcal{U}(0, 100)$	$\mathcal{U}(0, 100)$	$\mathcal{U}(0, 100)$	–	$\mathcal{U}(0, 100)$
$\sigma_{\text{dSHO,H-post}}$	$\mathcal{U}(0, 100)$	$\mathcal{U}(0, 100)$	$\mathcal{U}(0, 100)$	–	$\mathcal{U}(0, 100)$
$\sigma_{\text{dSHO,H-warmup}}$	–	–	–	$\mathcal{U}(0, 100)$	$\mathcal{U}(0, 100)$
$\sigma_{\text{dSHO,carnemes}}$	–	–	–	–	$\mathcal{U}(0, 100)$
$\sigma_{\text{QP,H-pre}}$	$\mathcal{U}(0, 100)$	$\mathcal{U}(0, 100)$	$\mathcal{U}(0, 100)$	–	$\mathcal{U}(0, 100)$
$\sigma_{\text{QP,H-post}}$	$\mathcal{U}(0, 100)$	$\mathcal{U}(0, 100)$	$\mathcal{U}(0, 100)$	–	$\mathcal{U}(0, 100)$
$\sigma_{\text{QP,H-warmup}}$	–	–	–	$\mathcal{U}(0, 100)$	$\mathcal{U}(0, 100)$
$\sigma_{\text{QP,carnemes}}$	–	–	–	–	$\mathcal{U}(0, 100)$
K_1	$\mathcal{U}(0, 50)$	$\mathcal{U}(0, 50)$	$\mathcal{U}(0, 50)$	$\mathcal{U}(0, 50)$	$\mathcal{U}(0, 50)$
P_1	$\mathcal{U}(1000, 10000)$	$\mathcal{U}(1, 10)$	$\mathcal{U}(8, 20)$	$\mathcal{U}(8, 20)$	$\mathcal{U}(8, 20)$
$\sqrt{e_1} \cos \omega_1$	$\mathcal{U}(-1, 1), \mathcal{F}(0)$	$\mathcal{U}(-1, 1), \mathcal{F}(0)$	$\mathcal{U}(-1, 1), \mathcal{F}(0)$	$\mathcal{U}(-1, 1), \mathcal{F}(0)$	$\mathcal{U}(-1, 1), \mathcal{F}(0)$
$\sqrt{e_1} \sin \omega_1$	$\mathcal{U}(-1, 1), \mathcal{F}(0)$	$\mathcal{U}(-1, 1), \mathcal{F}(0)$	$\mathcal{U}(-1, 1), \mathcal{F}(0)$	$\mathcal{U}(-1, 1), \mathcal{F}(0)$	$\mathcal{U}(-1, 1), \mathcal{F}(0)$
$t_{0,1}$	$\mathcal{U}(2455200, 2456500)$	$\mathcal{U}(2455200, 2455300)$	$\mathcal{U}(2459200, 2459220)$	$\mathcal{U}(2459200, 2459220)$	$\mathcal{U}(2459200, 2459117)$
K_2	$\mathcal{U}(0, 50)$	$\mathcal{U}(0, 50)$	$\mathcal{U}(0, 50)$	$\mathcal{U}(0, 50)$	$\mathcal{U}(0, 50)$
P_2	$\mathcal{U}(1, 1000)$	$\mathcal{U}(10, 100)$	$\mathcal{U}(1, 7)$	$\mathcal{U}(1, 7)$	$\mathcal{U}(1, 7)$
$\sqrt{e_2} \cos \omega_2$	$\mathcal{U}(-1, 1), \mathcal{F}(0)$	$\mathcal{U}(-1, 1), \mathcal{F}(0)$	$\mathcal{U}(-1, 1), \mathcal{F}(0)$	$\mathcal{U}(-1, 1), \mathcal{F}(0)$	$\mathcal{U}(-1, 1), \mathcal{F}(0)$
$\sqrt{e_2} \sin \omega_2$	$\mathcal{U}(-1, 1), \mathcal{F}(0)$	$\mathcal{U}(-1, 1), \mathcal{F}(0)$	$\mathcal{U}(-1, 1), \mathcal{F}(0)$	$\mathcal{U}(-1, 1), \mathcal{F}(0)$	$\mathcal{U}(-1, 1), \mathcal{F}(0)$
$t_{0,2}$	$\mathcal{U}(2455000, 2456000)$	$\mathcal{U}(2457300, 2457400)$	$\mathcal{U}(2459100, 2459107)$	$\mathcal{U}(2459100, 2459107)$	$\mathcal{U}(2459100, 2459107)$

Notes. The parameters are separated into seasonal instrumental, global GP, seasonal GP, Planet 1, and Planet 2 related groups. Not all parameters were in use for all models of a specific dataset. See Table F.1.

Appendix G: Model comparison posteriors

Appendix H: Additional Figures

In this section of the appendix we present additional figures that relate to topics discussed in the main text. We present the window function for the HARPS observations in Figs. H.1–H.3 and the best fitting model and residuals from the MCMC inference for Ross 128 incorporating CARMENES data in Sect. 5.1.3 in Fig. H.4. The full corner plots for each model presented in Table 5 (except the RedDots data only column) are shown in Figs. H.5–H.8. We show the periodogram of the $H\alpha$ activity indicator for Ross 128 in Fig. H.9. Figure H.10 illustrates the multiple peaks in the period posterior encountered for Ross 128. photometric time series for GJ 674 and Ross 128 are given in Figs. H.11 and H.12 and the corresponding GLS periodograms in Figs. H.13 and H.14. The detection limit grids for GJ 832 and GJ 674 from Sect. 5.3 are shown in Figs. H.15 and H.16, the comparison between the striping observed in Sect. 5.3 and the residual GLS power is given in Fig. H.17 and the mean of the residuals for the white noise realizations of Ross 128 in Fig. H.18. Figure H.19 shows the presence detection grids for GJ 832, GJ 674, and Ross 128 extended for very long periods.

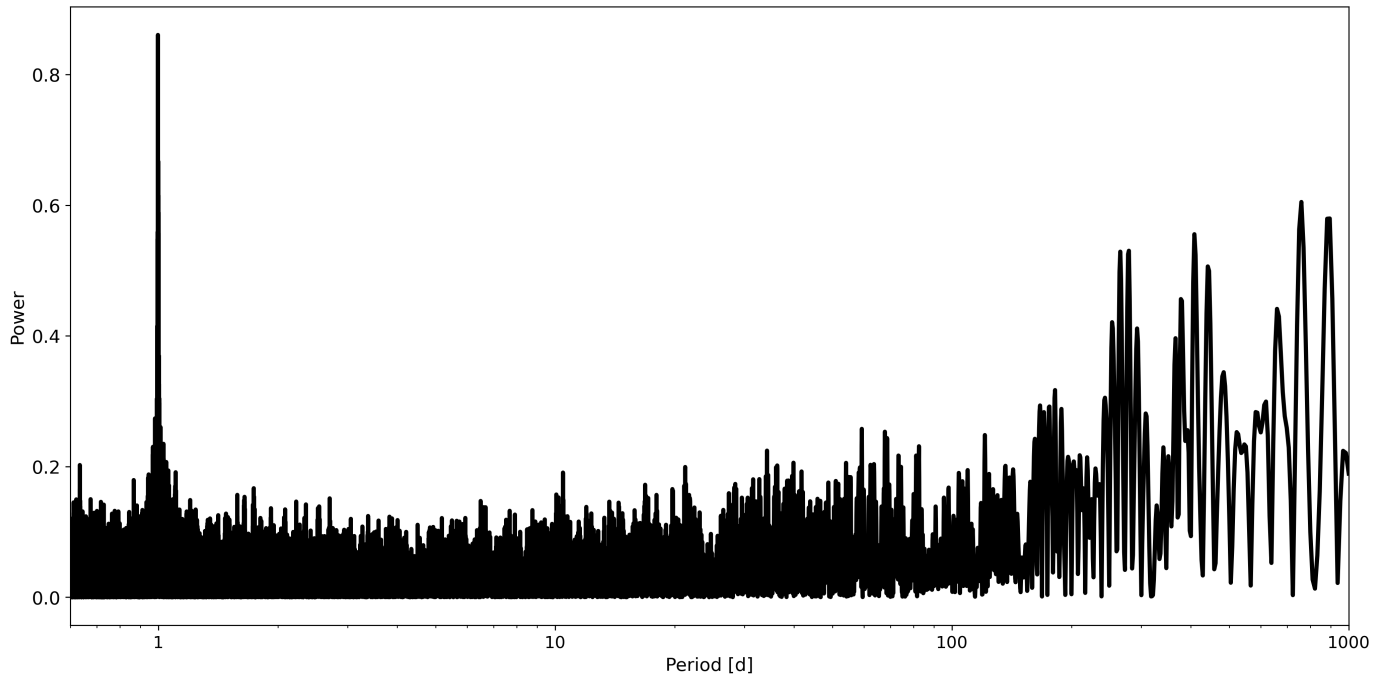


Fig. H.1. The window function from the GJ 832 HARPS observations. Besides the one day and one year periods, no strong periodicities are visible.

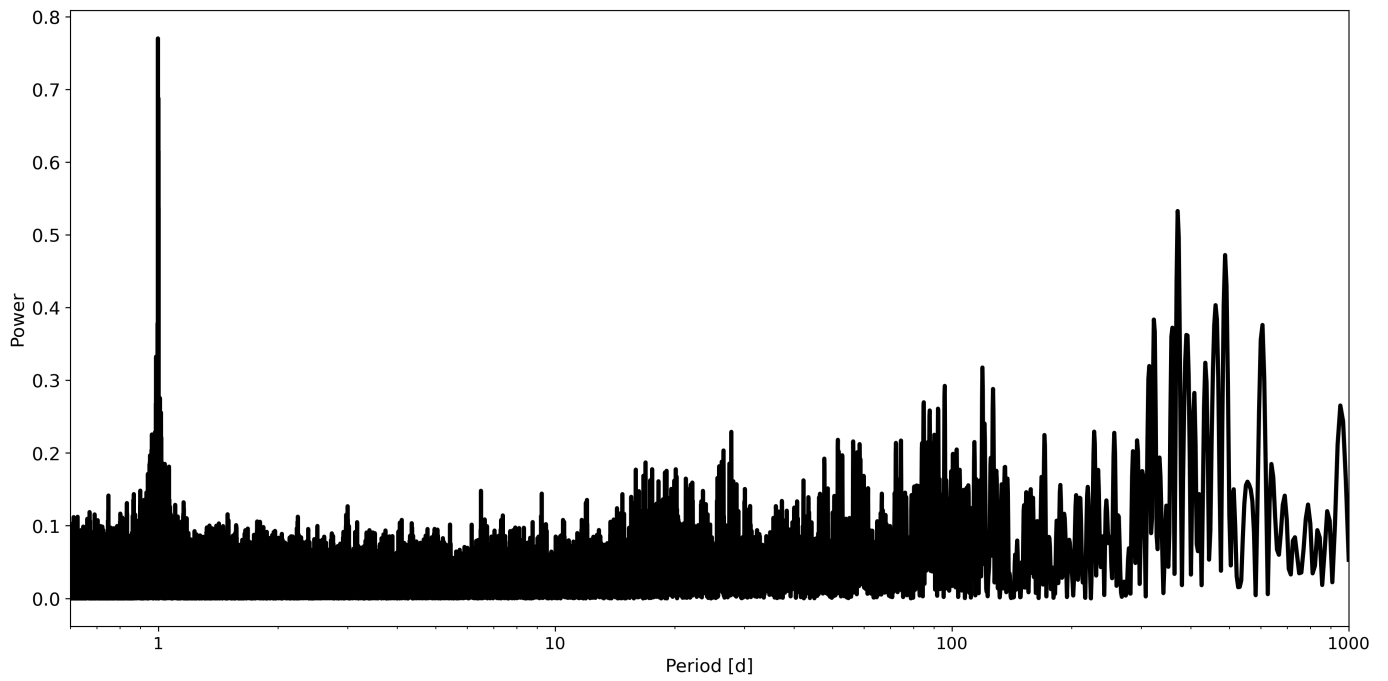


Fig. H.2. The window function from the GJ 674 HARPS observations. Besides the one day and one year periods, no strong periodicities are visible.

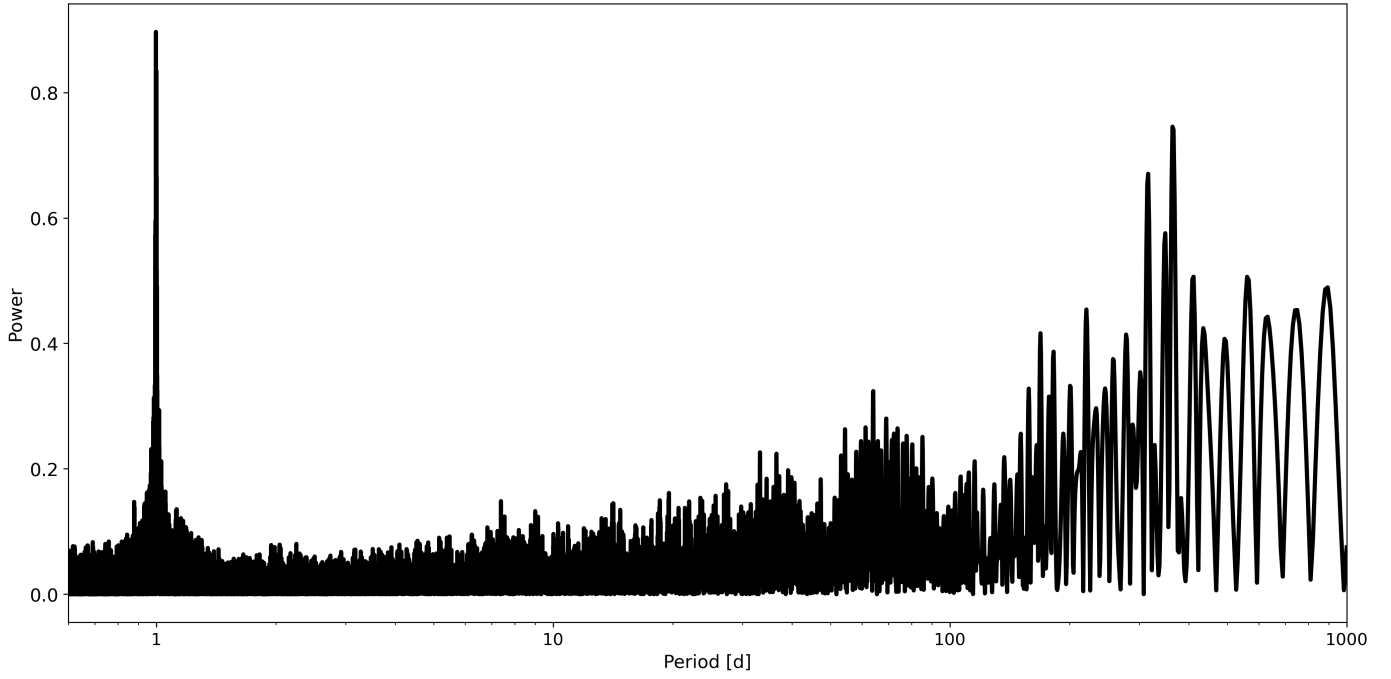


Fig. H.3. The window function from the Ross 128 HARPS observations. Besides the one day and one year periods, no strong periodicities are visible.

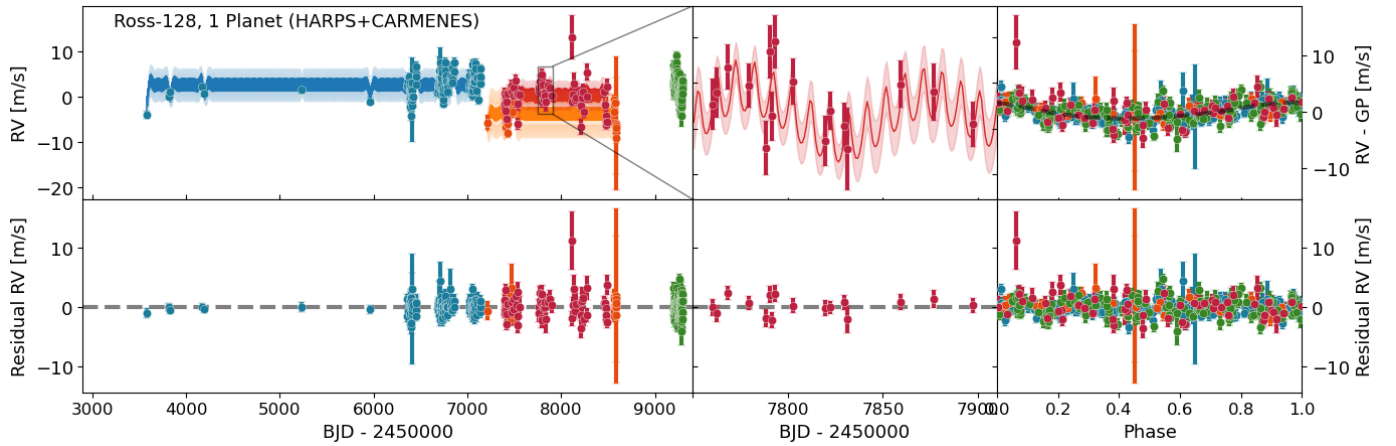


Fig. H.4. *Left:* Best fit of the 1 eccentric planet + GP-SHO model (which includes instrumental offsets) for Ross 128 (top) and the residuals (bottom). The model and RV data are separated by a small difference in color shade and the uncertainty of the model fit indicated by the more transparent region. The colors indicate the pre-fiber change (blue), post-fiber change (orange), and post-warmup (green) HARPS instrument seasons and the CARMENES data (red). The model parameters can be found in Table 5. The gray box marks the extent of the zoomed sub-panel. *Middle:* Zoom into the region of densest CARMENES observations marked by the gray box in the left panel. *Right:* Phase folded, activity subtracted, and instrumental offset corrected RV.

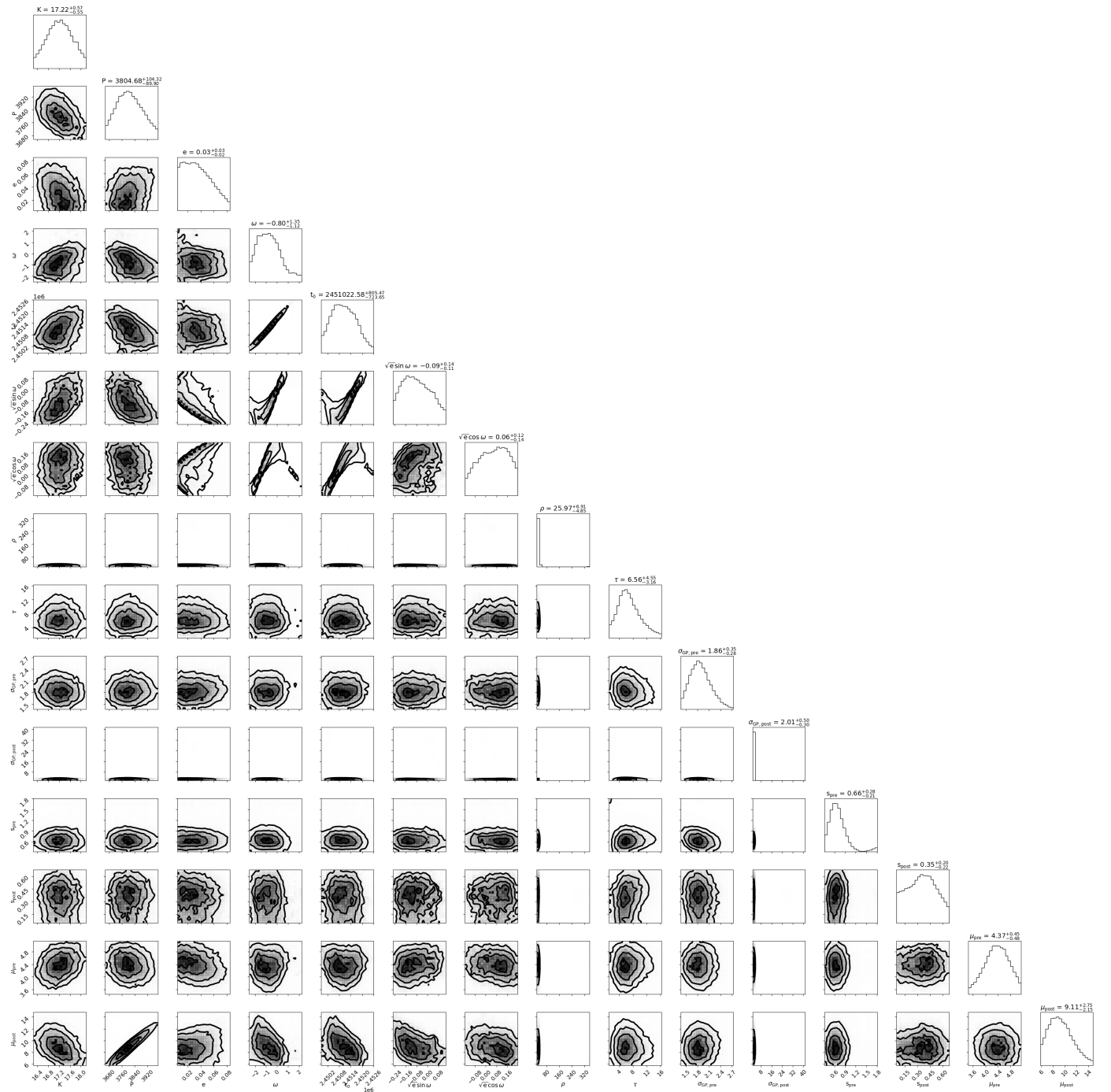


Fig. H.5. Corner contour and histogram plot for all MCMC derived parameters for the GJ 832 system from the last 5 000 steps for the one eccentric planet + GP-SHO model. The plotted ranges are limited to exclude the lowest 10 percentiles (see. Sect. 4.4.2). The inferred parameters are given in Table 5.

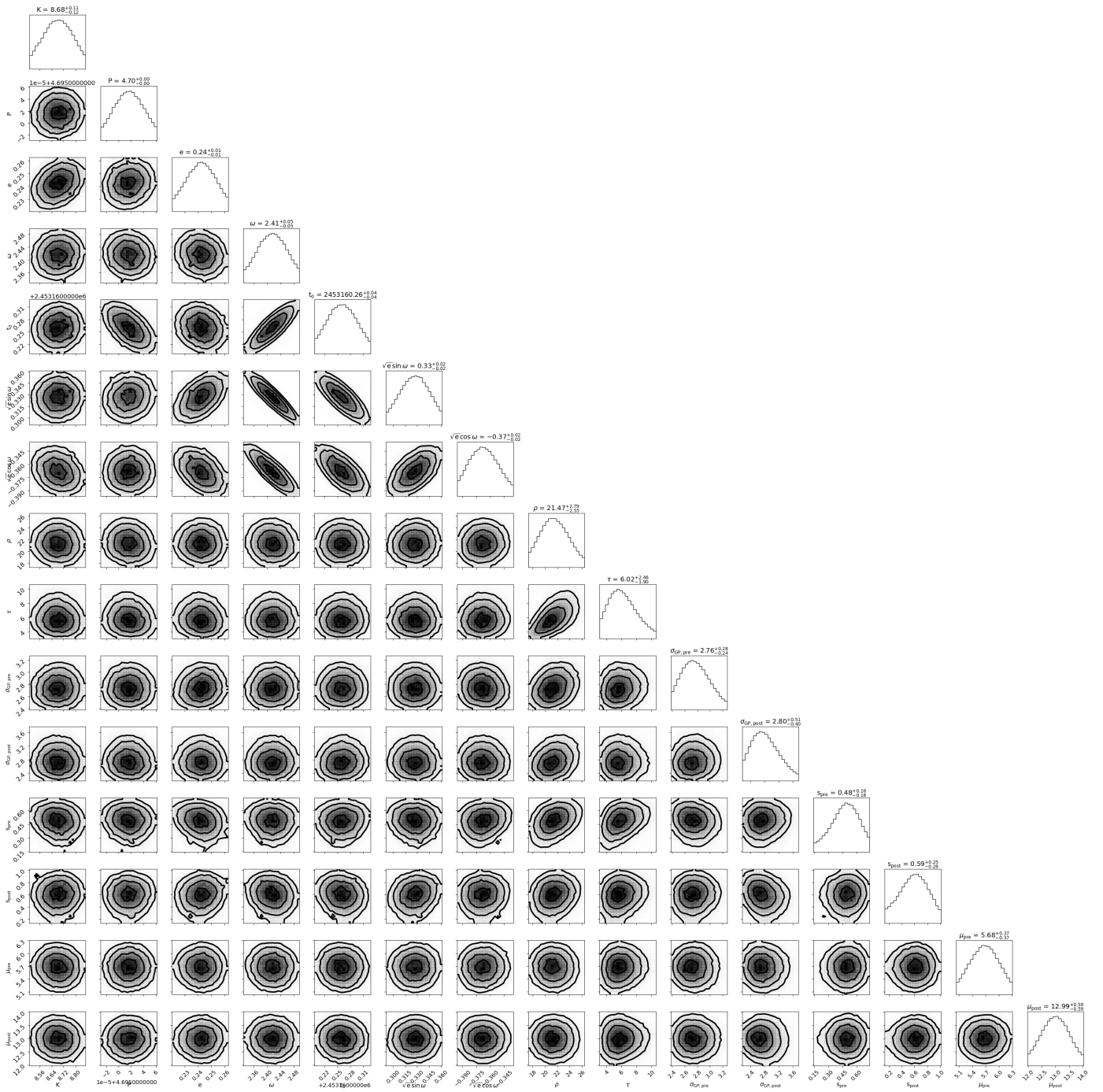


Fig. H.6. Corner contour and histogram plot for all MCMC derived parameters for the GJ 674 system from the last 5 000 steps for the one eccentric planet + GP-SHO model. The plotted ranges are limited to exclude the lowest 10 percentiles (see. Sect. 4.4.2). The inferred parameters are given in Table 5.

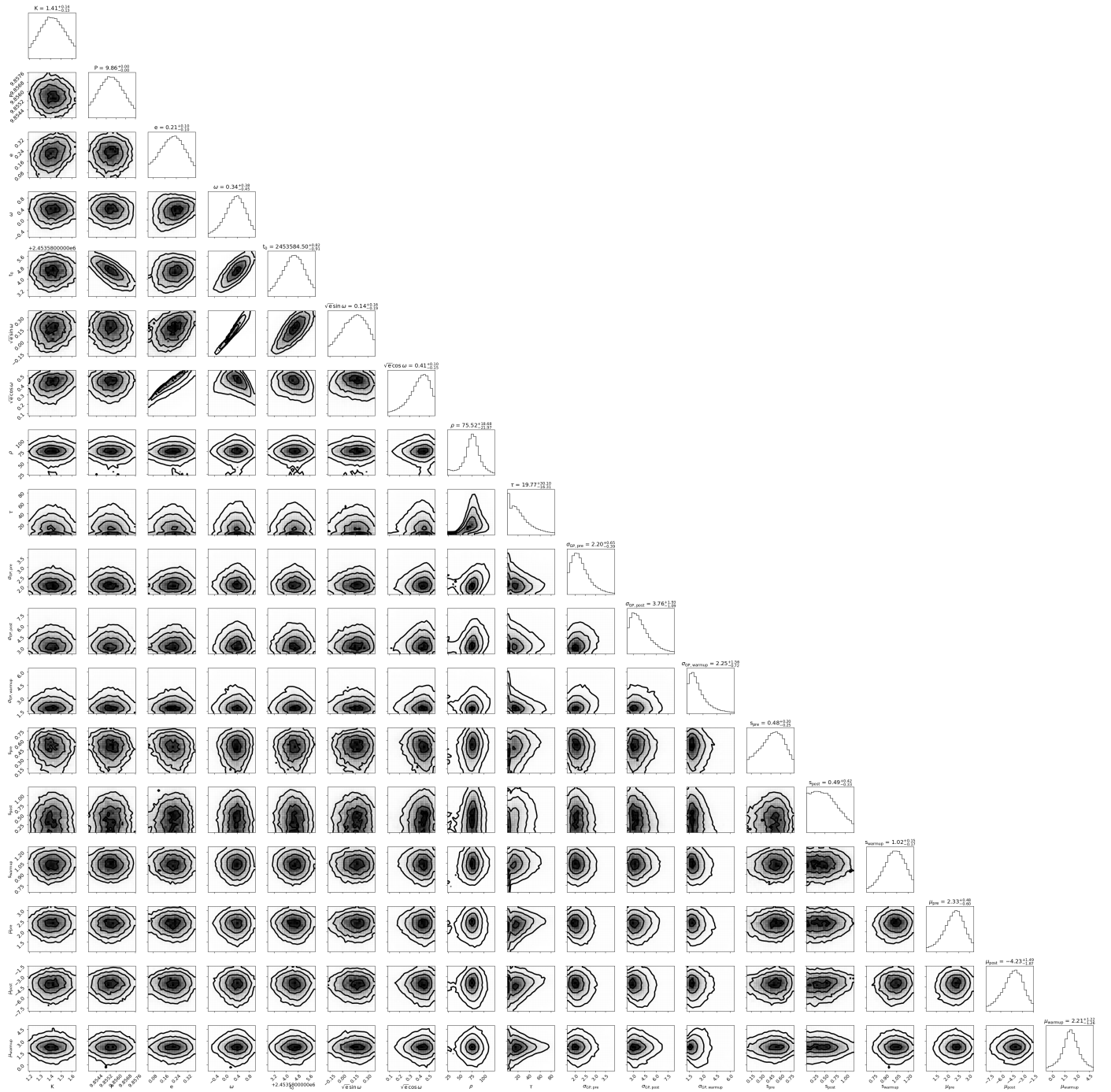


Fig. H.7. Corner contour and histogram plot for all MCMC derived parameters for the Ross 128 system using only HARPS data from the last 5 000 steps for the one eccentric planet + GP-SHO model. The plotted ranges are limited to exclude the lowest 10 percentiles (see. Sect. 4.4.2). The inferred parameters are given in Table 5.

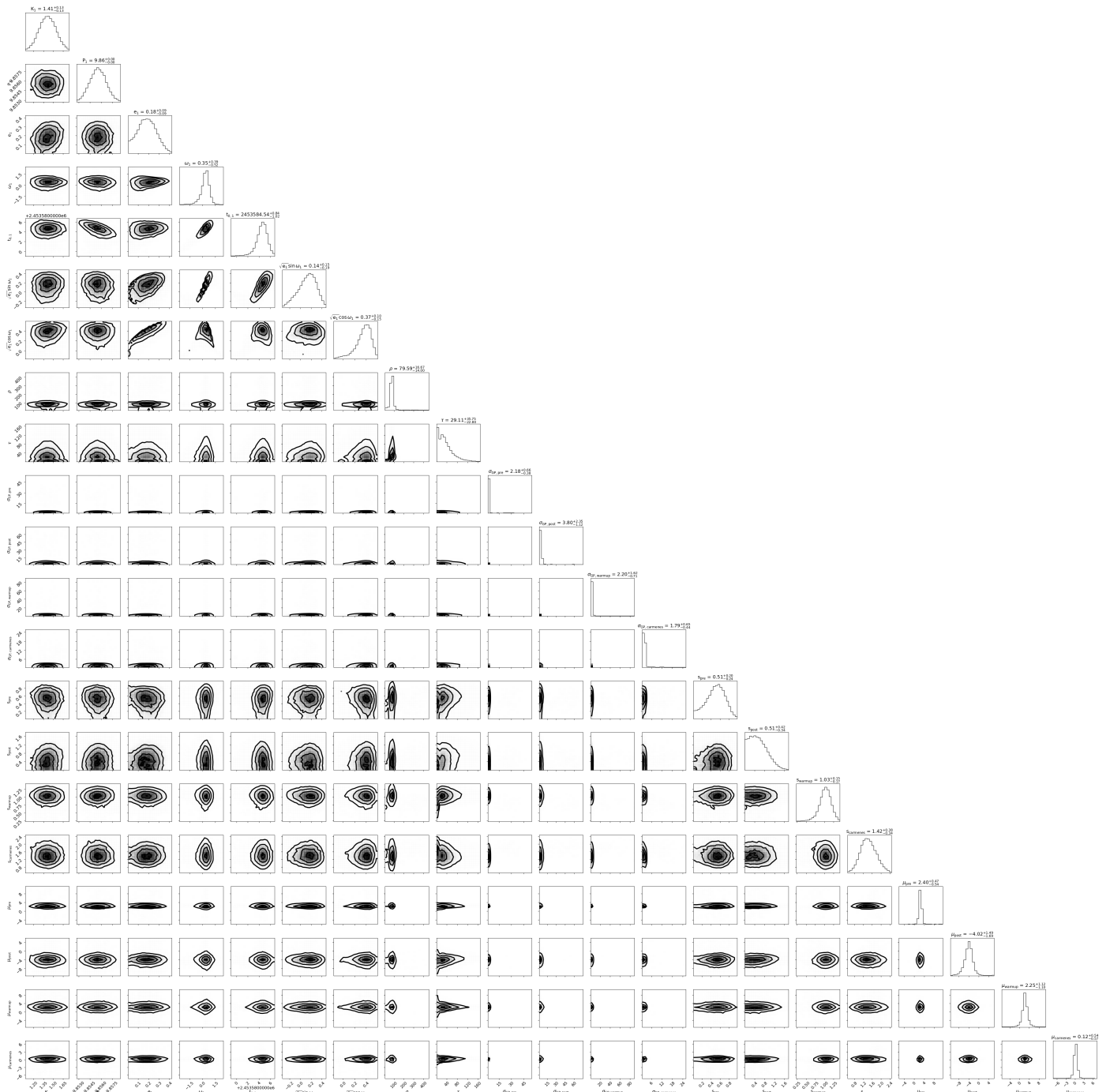


Fig. H.8. Corner contour and histogram plot for all MCMC derived parameters for the Ross 128 system using HARPS and CARMENES data from the last 5 000 steps for the one eccentric planet + GP-SHO model. The plotted ranges are limited to exclude the lowest 10 percentiles (see Sect. 4.4.2). The inferred parameters are given in Table 5.

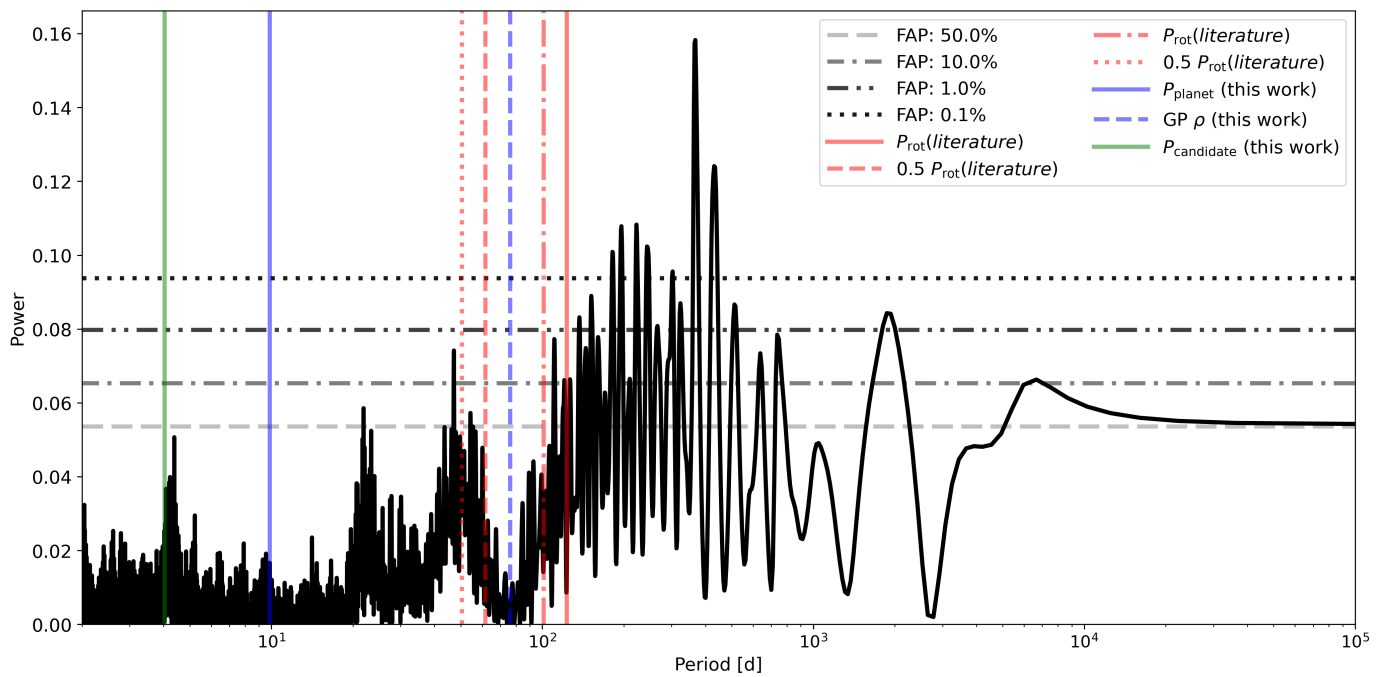


Fig. H.9. GLS periodogram of the $H\alpha$ activity indicator for Ross 128. Horizontal lines mark the false-alarm probability levels shown in the figure legend. Vertical lines mark the inferred (solid blue) planetary period P_{planet} , literature rotation period P_{rot} (solid red), half period (red dashed), alternative literature rotation periods $P_{\text{rot,alt}}$ (red dotted; see Table 1), and GP periods ρ (blue dashed).

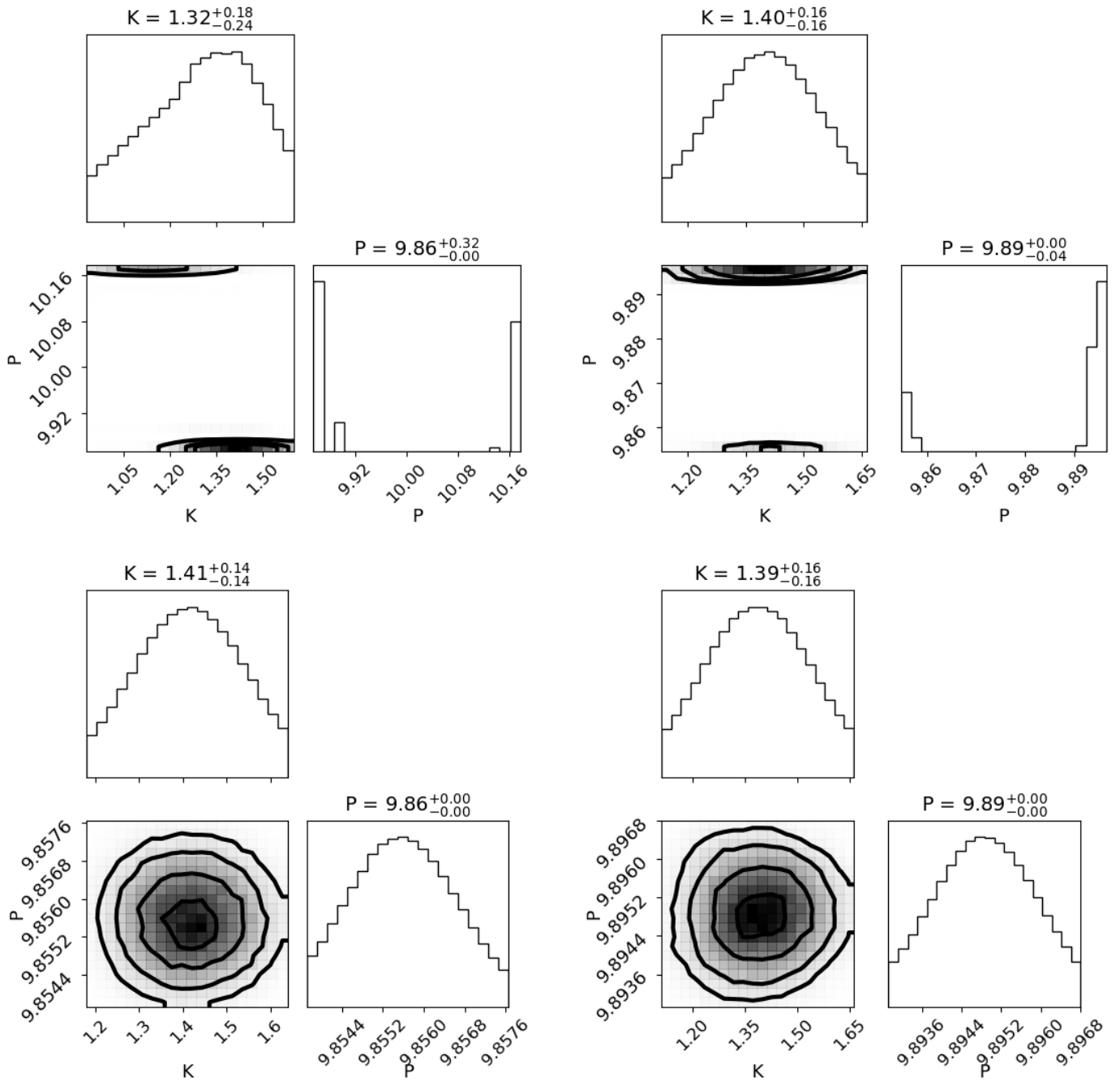


Fig. H.10. Successive zoom into the Ross 128 period posterior from the initial triple peak to the accepted primary peak. The only change between the panels is the width of the prior used for the period from very wide (Top Left; showing all three peaks), narrower (Top Right; removing 10.1 d peak) and very narrow (Bottom; Zoomed to 9.86 d [left] and 9.89 d [right]). The plotted ranges are limited to exclude the lowest 10 percentiles for illustration purposes (see Sect. 4.4.2)

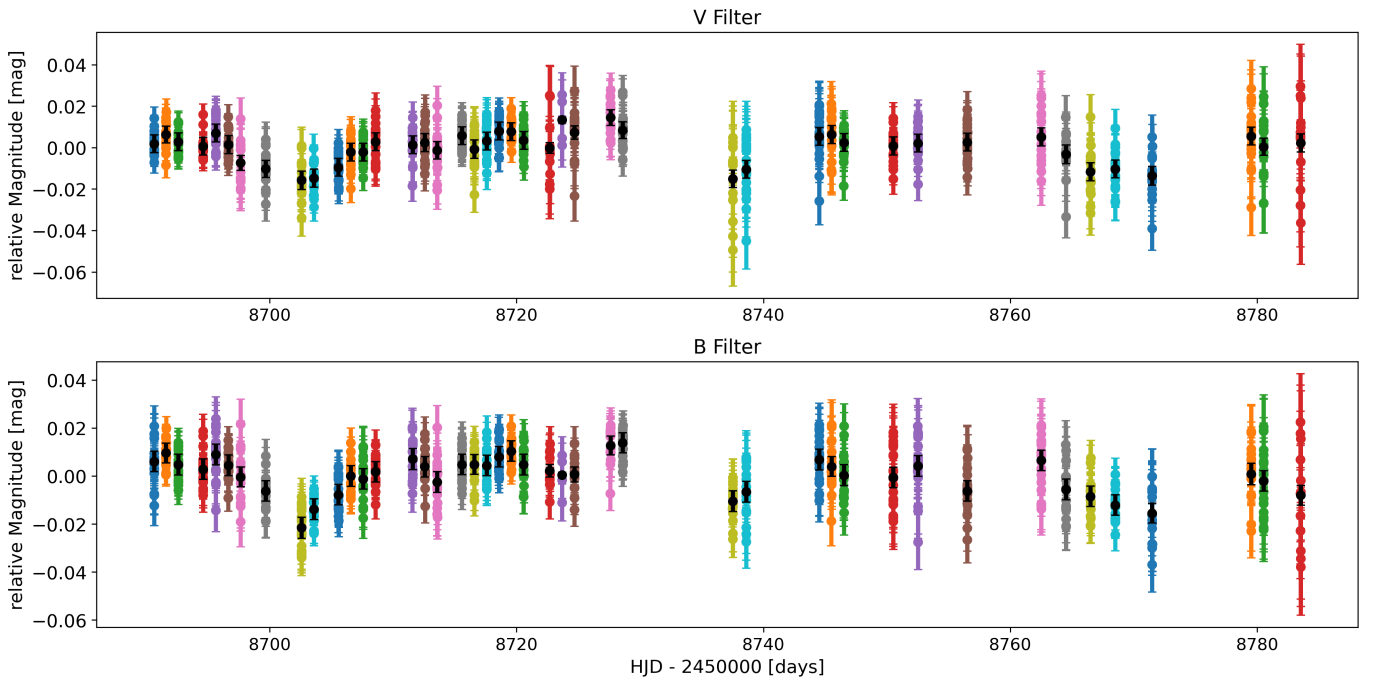


Fig. H.11. Nightly averaged, photometric timeseries of GJ 674, observed by the ASH2 telescope. Each nights individual observations are given (colored) with nightly averages plotted on top (black).

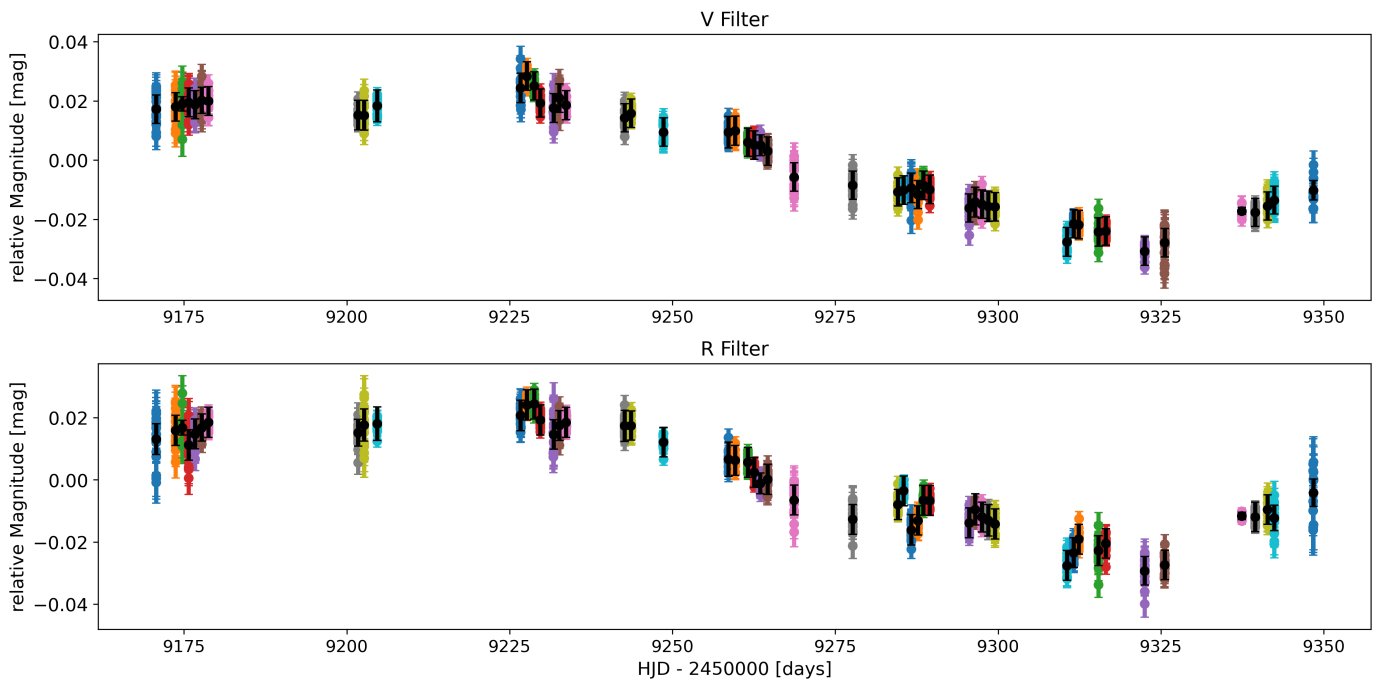


Fig. H.12. Nightly averaged, photometric timeseries of Ross 128, observed by the T90 telescope. Each nights individual observations are given (colored) with nightly averages plotted on top (black).

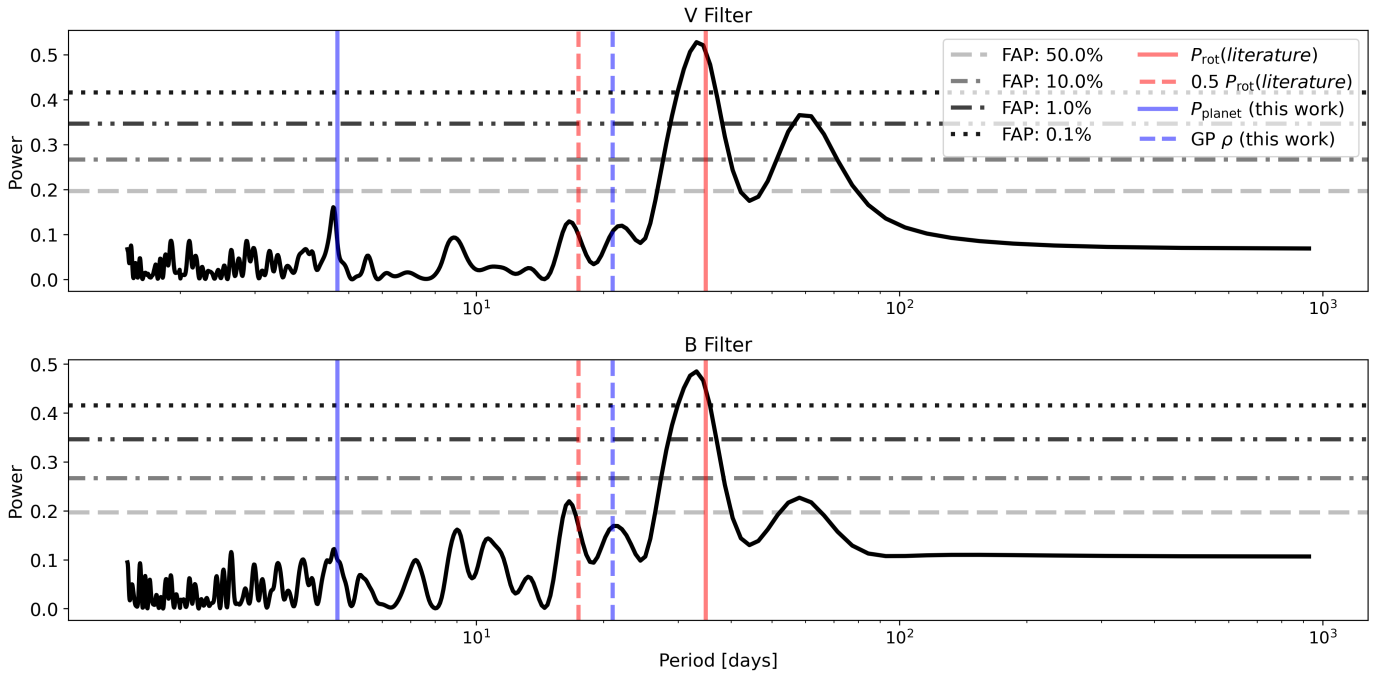


Fig. H.13. GLS periodogram of the nightly averaged, photometric timeseries of GJ 674. Vertical lines mark the inferred (solid blue) planetary period of $P_{\text{planet}} = 4.69 d$, literature rotation period P_{rot} (solid red), half period (red dashed), and GP periods ρ (blue dashed). The planetary orbital period matches the peak in the V Band.

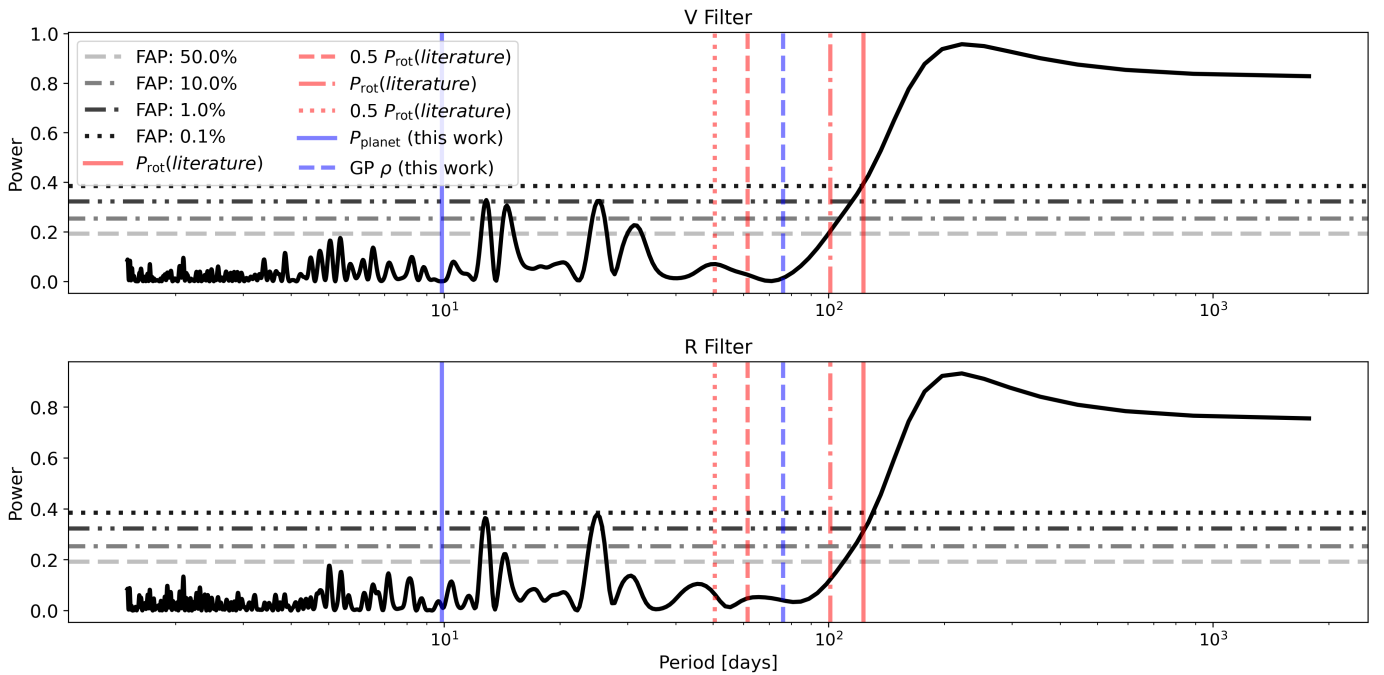


Fig. H.14. GLS periodogram of the nightly averaged, photometric timeseries of Ross 128. Vertical lines mark the inferred (solid blue) planetary period P_{planet} , literature rotation period P_{rot} (solid red), half period (red dashed), alternative literature rotation periods $P_{\text{rot,alt}}$ (red dotted; see Table 1), and GP periods ρ (blue dashed).

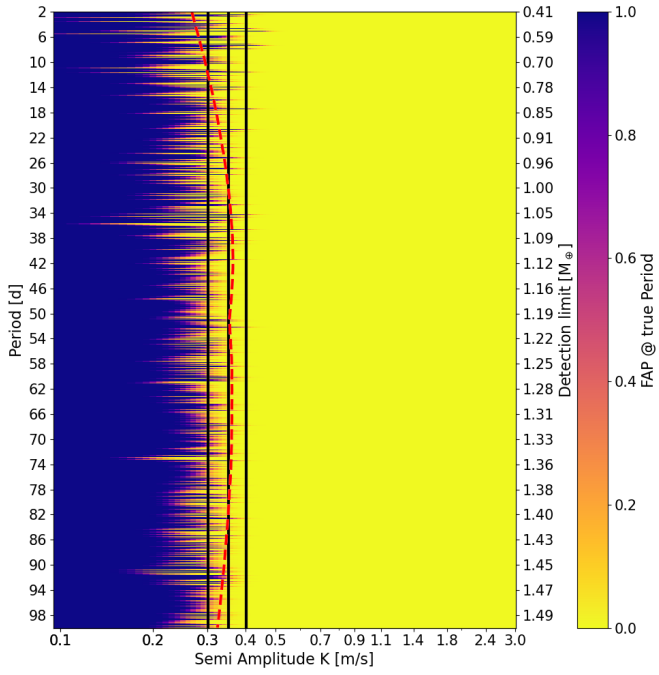


Fig. H.15. Grid of detections from GLS periodograms for planetary signals injected into the GJ 832 residual RVs. The median detection boundary is marked (black line) and the grid colored for the false-alarm-probability at the true, injected period.

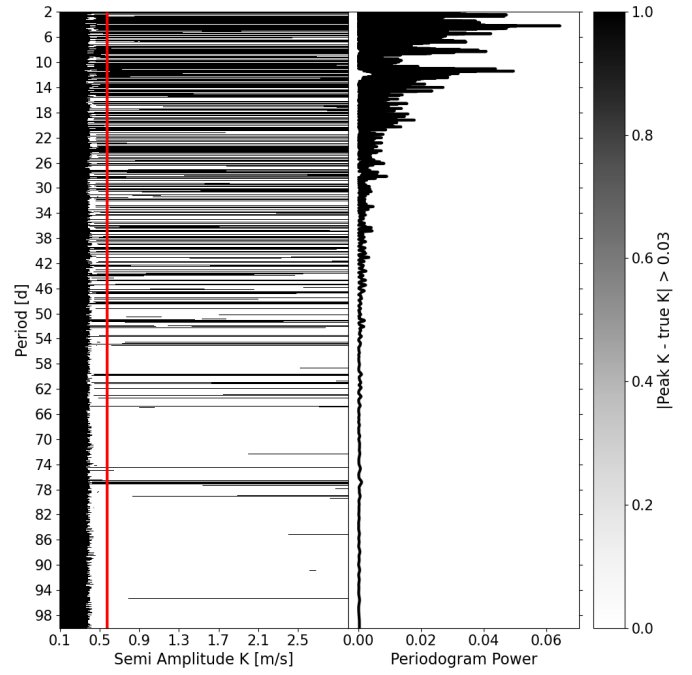


Fig. H.17. Comparing the GLS grid striped offsets in peak amplitudes (left) for Ross 128 injection models to residual power in the "noise" time series without the injected signal (right).

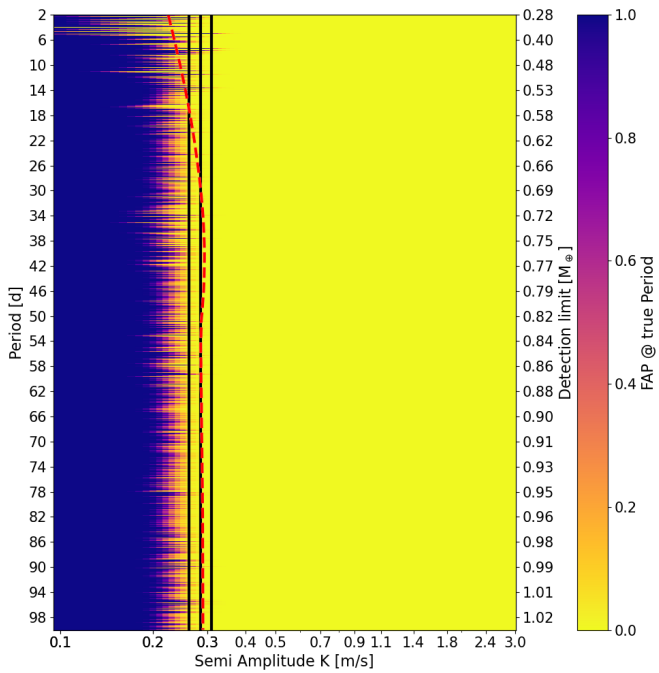


Fig. H.16. Grid of detections from GLS periodograms for planetary signals injected into the GJ 674 residual RVs. The median detection boundary is marked (black line) and the grid colored for the false-alarm-probability at the true, injected period.

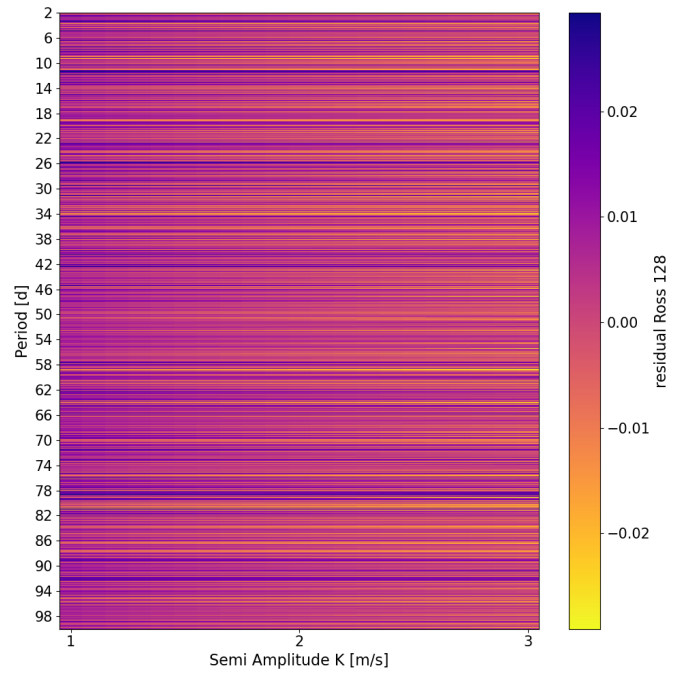


Fig. H.18. Average of 100 white noise realizations matching Ross 128 RV uncertainties with the true amplitude subtracted from the recovered value. The striping visible in Figs. 10, middle panel, and individual realizations is almost fully averaged out in the region of accepted detections (compare Fig. 10, left panel).

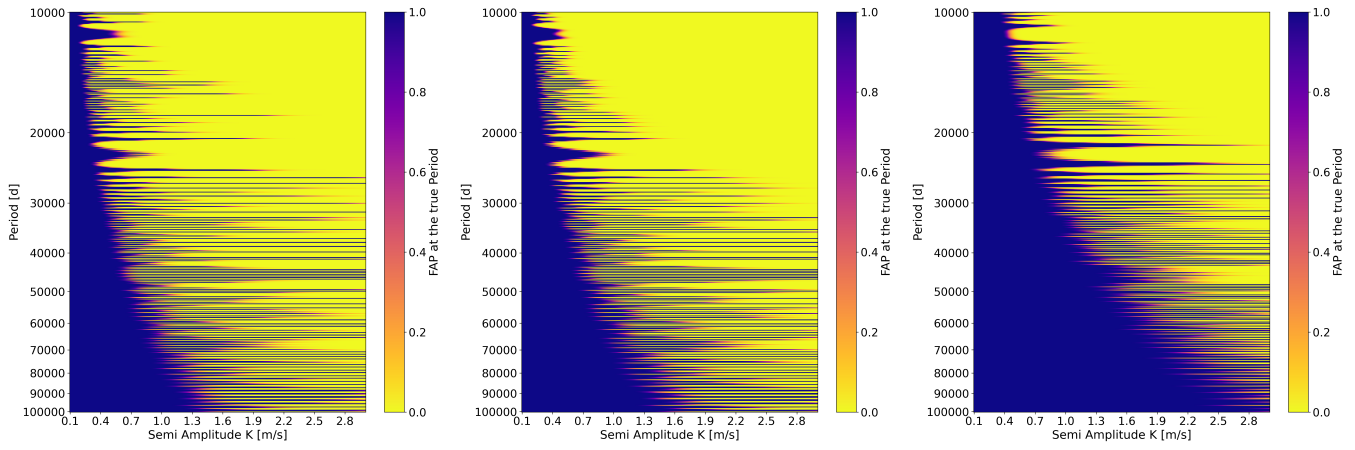


Fig. H.19. Grid of detections from GLS periodograms for planetary signals injected into the residual RVs of GJ 832 (left), GJ 674 (middle), and Ross 128 (right) for very long orbital periods.

Table G.6. Bayesian posteriors for the instrumental correction parameters obtained during the model comparison.

		$\mu_{H\text{-pre}}$	$\mu_{H\text{-post}}$	$\mu_{H\text{-warmup}}$	μ_{Carmenes}	$\sigma_{H\text{-pre}}$	$\sigma_{H\text{-post}}$	$\sigma_{H\text{-warmup}}$	σ_{Carmenes}
GJ 832 HARPS	OP	-1.2 ^{+1.3} _{-1.3}	9.86 ^{+0.11} _{-0.23}	-	-	10.4 ^{+1.0} _{-0.9}	10.9 ^{+0.7} _{-0.7}	-	-
GJ 674 HARPS	OP	6.4 ^{+0.5} _{-0.5}	9.86 ^{+0.11} _{-0.22}	-	-	6.7 ^{+0.4} _{-0.3}	7.8 ^{+0.7} _{-0.5}	-	-
Ross 128 HARPS	OP	2.62 ^{+0.20} _{-0.20}	-2.8 ^{+0.6} _{-0.6}	1.75 ^{+0.21} _{-0.21}	-	2.04 ^{+0.16} _{-0.15}	3.0 ^{+0.5} _{-0.4}	2.24 ^{+0.18} _{-0.16}	-
Ross 128 RedDots	OP	-	-	1.75 ^{+0.21} _{-0.22}	-	-	-	2.23 ^{+0.18} _{-0.16}	-
Ross 128 HARPS+Carmenes	OP	2.62 ^{+0.20} _{-0.20}	-2.8 ^{+0.6} _{-0.6}	1.75 ^{+0.22} _{-0.21}	-0.1 ^{+0.4} _{-0.4}	2.05 ^{+0.17} _{-0.17}	3.0 ^{+0.5} _{-0.4}	2.24 ^{+0.17} _{-0.17}	2.6 ^{+0.3} _{-0.3}
GJ 832 HARPS	IP ^{ecc}	4.2 ^{+0.4} _{-0.4}	8.9 ^{+0.7} _{-1.2}	-	-	1.89 ^{+0.21} _{-0.18}	1.84 ^{+0.16} _{-0.15}	-	-
GJ 674 HARPS	IP ^{ecc}	5.91 ^{+0.22} _{-0.22}	9.95 ^{+0.04} _{-0.09}	-	-	2.82 ^{+0.16} _{-0.15}	4.0 ^{+0.4} _{-0.3}	-	-
Ross 128 HARPS	IP ^{ecc}	2.73 ^{+0.18} _{-0.18}	-3.0 ^{+0.5} _{-0.5}	1.71 ^{+0.20} _{-0.19}	-	1.76 ^{+0.15} _{-0.14}	2.5 ^{+0.5} _{-0.4}	2.04 ^{+0.17} _{-0.16}	-
Ross 128 RedDots	IP ^{ecc}	-	-	1.76 ^{+0.20} _{-0.20}	-	-	-	2.03 ^{+0.18} _{-0.17}	-
Ross 128 HARPS+Carmenes	IP ^{ecc}	2.74 ^{+0.18} _{-0.18}	-3.0 ^{+0.5} _{-0.5}	1.70 ^{+0.20} _{-0.20}	-0.2 ^{+0.4} _{-0.3}	1.75 ^{+0.15} _{-0.14}	2.5 ^{+0.4} _{-0.4}	2.05 ^{+0.17} _{-0.16}	2.2 ^{+0.3} _{-0.3}
GJ 832 HARPS	IP ^{citr}	4.3 ^{+0.3} _{-0.3}	8.96 ^{+0.72} _{-0.99}	-	-	1.88 ^{+0.21} _{-0.18}	1.84 ^{+0.16} _{-0.15}	-	-
GJ 674 HARPS	IP ^{citr}	5.92 ^{+0.23} _{-0.23}	9.95 ^{+0.04} _{-0.09}	-	-	3.01 ^{+0.18} _{-0.17}	4.1 ^{+0.4} _{-0.3}	-	-
Ross 128 HARPS	IP ^{citr}	2.74 ^{+0.18} _{-0.18}	-2.9 ^{+0.5} _{-0.5}	1.70 ^{+0.20} _{-0.19}	-	1.75 ^{+0.15} _{-0.14}	2.5 ^{+0.5} _{-0.4}	2.06 ^{+0.17} _{-0.16}	-
Ross 128 RedDots	IP ^{citr}	-	-	1.70 ^{+0.20} _{-0.20}	-	-	-	2.06 ^{+0.17} _{-0.16}	-
Ross 128 HARPS+Carmenes	IP ^{citr}	2.74 ^{+0.18} _{-0.18}	-2.9 ^{+0.5} _{-0.5}	1.70 ^{+0.20} _{-0.20}	-0.2 ^{+0.4} _{-0.3}	1.75 ^{+0.15} _{-0.14}	2.4 ^{+0.5} _{-0.4}	2.05 ^{+0.17} _{-0.16}	2.2 ^{+0.3} _{-0.3}
GJ 832 HARPS	2P ^{ecc}	4.20 ^{+0.22} _{-0.22}	8.2 ^{+1.3} _{-0.9}	-	-	1.9 ^{+0.3} _{-0.3}	2.10 ^{+0.22} _{-0.28}	-	-
GJ 674 HARPS	2P ^{ecc}	6.05 ^{+0.17} _{-0.17}	9.95 ^{+0.04} _{-0.08}	-	-	2.13 ^{+0.14} _{-0.13}	3.8 ^{+0.4} _{-0.4}	-	-
Ross 128 HARPS	2P ^{ecc}	2.95 ^{+0.03} _{-0.06}	-1.26 ^{+0.07} _{-0.07}	1.895 ^{+0.017} _{-0.013}	-	1.611 ^{+0.011} _{-0.018}	4.22 ^{+0.05} _{-0.10}	2.257 ^{+0.012} _{-0.013}	-
Ross 128 RedDots	2P ^{ecc}	-	-	1.43 ^{+0.09} _{-0.09}	-	-	-	2.12 ^{+0.04} _{-0.04}	-
Ross 128 HARPS+Carmenes	2P ^{ecc}	2.947 ^{+0.010} _{-0.011}	-2.88 ^{+0.03} _{-0.03}	1.287 ^{+0.021} _{-0.019}	0.117 ^{+0.021} _{-0.047}	2.051 ^{+0.004} _{-0.007}	2.746 ^{+0.021} _{-0.029}	2.645 ^{+0.009} _{-0.016}	2.36 ^{+0.08} _{-0.04}
GJ 832 HARPS	2P ^{citr}	4.17 ^{+0.33} _{-0.18}	8.3 ^{+1.1} _{-0.6}	-	-	1.63 ^{+0.19} _{-0.16}	1.64 ^{+0.22} _{-0.16}	-	-
GJ 674 HARPS	2P ^{citr}	6.06 ^{+0.19} _{-0.20}	9.95 ^{+0.04} _{-0.09}	-	-	2.46 ^{+0.15} _{-0.14}	3.7 ^{+0.4} _{-0.3}	-	-
Ross 128 HARPS	2P ^{citr}	2.67 ^{+0.16} _{-0.16}	-2.6 ^{+0.4} _{-0.5}	1.77 ^{+0.17} _{-0.17}	-	2.06 ^{+0.15} _{-0.15}	2.8 ^{+0.5} _{-0.4}	1.99 ^{+0.16} _{-0.15}	-
Ross 128 RedDots	2P ^{citr}	-	-	1.83 ^{+0.15} _{-0.15}	-	-	-	1.26 ^{+0.14} _{-0.13}	-
Ross 128 HARPS+Carmenes	2P ^{citr}	2.85 ^{+0.15} _{-0.08}	-3.12 ^{+0.25} _{-0.36}	1.80 ^{+0.12} _{-0.06}	-0.05 ^{+0.05} _{-0.06}	2.29 ^{+0.04} _{-0.06}	2.00 ^{+0.46} _{-0.18}	1.88 ^{+0.11} _{-0.07}	2.16 ^{+0.05} _{-0.08}
GJ 832 HARPS	OP + GP-SHO	4.4 ^{+0.5} _{-0.5}	9.4 ^{+0.3} _{-0.9}	-	-	1.86 ^{+0.20} _{-0.18}	1.82 ^{+0.16} _{-0.15}	-	-
GJ 674 HARPS	OP + GP-SHO	6.2 ^{+0.6} _{-0.6}	9.84 ^{+0.12} _{-0.25}	-	-	0.9 ^{+0.6} _{-0.5}	0.7 ^{+0.7} _{-0.5}	-	-
Ross 128 HARPS	OP + GP-SHO	2.2 ^{+0.5} _{-0.5}	-3.96 ^{+0.90} _{-0.97}	2.26 ^{+0.97} _{-0.99}	-	0.22 ^{+0.22} _{-0.15}	0.32 ^{+0.35} _{-0.22}	0.4 ^{+0.3} _{-0.3}	-
Ross 128 RedDots	OP + GP-SHO	-	-	2.3 ^{+1.3} _{-1.3}	-	-	-	0.27 ^{+0.25} _{-0.19}	-
Ross 128 HARPS+Carmenes	OP + GP-SHO	2.3 ^{+0.5} _{-0.5}	-4.0 ^{+0.9} _{-0.9}	2.3 ^{+0.9} _{-0.9}	0.2 ^{+0.6} _{-0.5}	0.23 ^{+0.23} _{-0.19}	0.32 ^{+0.35} _{-0.22}	0.4 ^{+0.3} _{-0.3}	1.2 ^{+0.5} _{-0.5}
GJ 832 HARPS	OP + GP-dHO	1.3 ^{+2.2} _{-2.3}	7.1 ^{+2.0} _{-3.0}	-	-	0.70 ^{+0.19} _{-0.17}	0.50 ^{+0.18} _{-0.21}	-	-
GJ 674 HARPS	OP + GP-dHO	5.92 ^{+0.23} _{-0.23}	9.94 ^{+0.05} _{-0.10}	-	-	2.6 ^{+0.2} _{-0.2}	3.7 ^{+0.6} _{-0.3}	-	-
Ross 128 HARPS	OP + GP-dHO	2.4 ^{+0.3} _{-0.4}	-3.9 ^{+0.8} _{-0.8}	2.2 ^{+0.8} _{-0.7}	-	0.34 ^{+0.29} _{-0.23}	0.4 ^{+0.4} _{-0.3}	0.60 ^{+0.25} _{-0.30}	-
Ross 128 RedDots	OP + GP-dHO	-	-	2.2 ^{+0.8} _{-0.8}	-	-	-	0.34 ^{+0.30} _{-0.23}	-
Ross 128 HARPS+Carmenes	OP + GP-dHO	2.4 ^{+0.3} _{-0.4}	-3.9 ^{+0.8} _{-0.8}	2.2 ^{+0.8} _{-0.8}	0.0 ^{+0.4} _{-0.4}	0.37 ^{+0.32} _{-0.25}	0.36 ^{+0.37} _{-0.25}	0.6 ^{+0.3} _{-0.3}	1.6 ^{+0.5} _{-0.5}
GJ 832 HARPS	OP + GP-QP	2 ⁺⁵ ₋₅	1 ⁺⁶ ₋₇	-	-	1.31 ^{+0.17} _{-0.15}	1.05 ^{+0.13} _{-0.13}	-	-
GJ 674 HARPS	OP + GP-QP	2 ⁺⁵ ₋₇	3 ⁺⁵ ₋₇	-	-	2.75 ^{+0.16} _{-0.16}	2.64 ^{+0.26} _{-0.24}	-	-
Ross 128 HARPS	OP + GP-QP	2.2 ^{+0.5} _{-0.5}	-3.9 ^{+1.1} _{-1.2}	2.2 ^{+1.1} _{-1.1}	-	0.4 ^{+0.3} _{-0.3}	0.4 ^{+0.4} _{-0.3}	0.87 ^{+0.17} _{-0.19}	-
Ross 128 RedDots	OP + GP-QP	-	-	2.2 ^{+0.6} _{-0.6}	-	-	-	0.4 ^{+0.3} _{-0.3}	-
Ross 128 HARPS+Carmenes	OP + GP-QP	2.2 ^{+0.5} _{-0.5}	-3.8 ^{+1.2} _{-1.2}	2.1 ^{+1.2} _{-1.1}	0.1 ^{+0.6} _{-0.6}	0.44 ^{+0.25} _{-0.25}	0.4 ^{+0.4} _{-0.3}	0.89 ^{+0.17} _{-0.18}	1.4 ^{+0.5} _{-0.4}

Table G.6. continued.

		$\mu_{\text{H-pre}}$	$\mu_{\text{H-post}}$	$\mu_{\text{H-warmup}}$	μ_{Carmenes}	$\sigma_{\text{H-pre}}$	$\sigma_{\text{H-post}}$	$\sigma_{\text{H-warmup}}$	σ_{Carmenes}
GJ 832 HARPS	IP _{ecc} + GP-SHO	4.4 ^{+0.4}	8.0 ^{+1.3}	—	—	0.55 ^{+0.22}	0.28 ^{+0.21}	—	—
GJ 674 HARPS	IP _{ecc} + GP-SHO	5.5 ^{+0.3}	9.84 ^{+0.7}	—	—	0.33 ^{+0.19}	0.6 ^{+0.3}	—	—
Ross 128 HARPS	IP _{ecc} + GP-SHO	2.0 ^{+0.3}	-4.7 ^{-0.9}	2.3 ^{+1.3}	—	0.26 ^{+0.20}	0.6 ^{+0.4}	0.81 ^{+0.17}	—
Ross 128 RedDots	IP _{ecc} + GP-SHO	—	—	2.0 ^{+1.1}	—	—	—	0.5 ^{+0.3}	—
Ross 128 HARPS+Carmenes	IP _{ecc} + GP-SHO	2.3 ^{+0.5}	-4.24 ^{+0.96}	2.1 ^{+1.2}	0.1 ^{+0.6}	0.25 ^{+0.22}	0.4 ^{+0.4}	0.79 ^{+0.17}	1.2 ^{+0.4}
GJ 832 HARPS	IP _{circ} + GP-SHO	4.5 ^{+0.3}	8.0 ^{+1.2}	—	—	0.56 ^{+0.32}	0.27 ^{+0.21}	—	—
GJ 674 HARPS	IP _{circ} + GP-SHO	5.7 ^{+0.3}	9.85 ^{+0.7}	—	—	1.63 ^{+0.3}	1.5 ^{+0.3}	—	—
Ross 128 HARPS	IP _{circ} + GP-SHO	2.3 ^{+0.6}	-4.2 ^{+1.0}	2.0 ^{+1.3}	—	0.28 ^{+0.19}	0.34 ^{+0.36}	0.79 ^{+0.18}	—
Ross 128 RedDots	IP _{circ} + GP-SHO	—	—	2.2 ^{+1.3}	—	—	—	0.5 ^{+0.3}	—
Ross 128 HARPS+Carmenes	IP _{circ} + GP-SHO	2.4 ^{+0.5}	-4.4 ^{+0.9}	2.4 ^{+1.2}	-0.0 ^{+0.6}	0.33 ^{+0.21}	0.35 ^{+0.33}	0.78 ^{+0.17}	1.2 ^{+0.4}
GJ 832 HARPS	IP _{ecc} + GP-dSHO	4.5 ^{+0.3}	8.1 ^{+1.2}	—	—	0.65 ^{+0.27}	0.33 ^{+0.20}	—	—
GJ 674 HARPS	IP _{ecc} + GP-dSHO	5.8 ^{+0.3}	9.88 ^{+0.9}	—	—	0.49 ^{+0.14}	0.44 ^{+0.25}	—	—
Ross 128 HARPS	IP _{ecc} + GP-dSHO	2.5 ^{+0.3}	-4.0 ^{+1.2}	2.2 ^{+0.8}	—	0.50 ^{+0.16}	0.5 ^{+0.26}	1.05 ^{+0.14}	—
Ross 128 RedDots	IP _{ecc} + GP-dSHO	—	—	2.3 ^{+1.0}	—	—	—	1.08 ^{+0.14}	—
Ross 128 HARPS+Carmenes	IP _{ecc} + GP-dSHO	2.5 ^{+0.4}	-4.0 ^{+1.0}	2.2 ^{+0.9}	0.2 ^{+0.4}	0.52 ^{+0.19}	0.6 ^{+0.4}	1.06 ^{+0.14}	1.4 ^{+0.3}
GJ 832 HARPS	IP _{circ} + GP-dSHO	4.5 ^{+0.3}	8.0 ^{+1.3}	—	—	0.65 ^{+0.27}	0.33 ^{+0.19}	—	—
GJ 674 HARPS	IP _{circ} + GP-dSHO	5.9 ^{+0.3}	9.85 ^{+0.7}	—	—	1.72 ^{+0.12}	1.37 ^{+0.20}	—	—
Ross 128 HARPS	IP _{circ} + GP-dSHO	2.5 ^{+0.4}	-4.0 ^{+1.3}	2.2 ^{+0.7}	—	0.59 ^{+0.14}	0.5 ^{+0.24}	1.07 ^{+0.14}	—
Ross 128 RedDots	IP _{circ} + GP-dSHO	—	—	2.1 ^{+0.7}	—	—	—	1.10 ^{+0.14}	—
Ross 128 HARPS+Carmenes	IP _{circ} + GP-dSHO	2.5 ^{+0.3}	-4.0 ^{+1.1}	2.2 ^{+0.7}	0.2 ^{+0.4}	0.60 ^{+0.17}	0.5 ^{+0.4}	1.06 ^{+0.13}	1.4 ^{+0.3}
GJ 832 HARPS	IP _{ecc} + GP-QP	4.4 ^{+0.4}	8.0 ^{+1.3}	—	—	0.65 ^{+0.28}	0.36 ^{+0.19}	—	—
GJ 674 HARPS	IP _{ecc} + GP-QP	5.7 ^{+0.6}	9.75 ^{+0.9}	—	—	0.67 ^{+0.12}	0.63 ^{+0.20}	—	—
Ross 128 HARPS	IP _{ecc} + GP-QP	2.2 ^{+0.5}	-4.4 ^{+1.5}	2.3 ^{+1.1}	—	0.53 ^{+0.18}	0.5 ^{+0.22}	1.06 ^{+0.14}	—
Ross 128 RedDots	IP _{ecc} + GP-QP	—	—	2.4 ^{+1.4}	—	—	—	1.03 ^{+0.14}	—
Ross 128 HARPS+Carmenes	IP _{ecc} + GP-QP	2.2 ^{+0.5}	-4.4 ^{+1.5}	2.3 ^{+0.8}	0.1 ^{+0.6}	0.56 ^{+0.19}	0.5 ^{+0.4}	1.06 ^{+0.13}	1.4 ^{+0.3}
GJ 832 HARPS	IP _{circ} + GP-QP	4.5 ^{+0.4}	7.9 ^{+1.3}	—	—	0.64 ^{+0.20}	0.36 ^{+0.19}	—	—
GJ 674 HARPS	IP _{circ} + GP-QP	4 ^{+0.4}	4 ^{+1.5}	—	—	2.69 ^{+0.16}	2.52 ^{+0.21}	—	—
Ross 128 HARPS	IP _{circ} + GP-QP	2.3 ^{+0.4}	-4.0 ^{+1.3}	2.5 ^{+0.9}	—	0.54 ^{+0.18}	0.5 ^{+0.15}	1.04 ^{+0.16}	—
Ross 128 RedDots	IP _{circ} + GP-QP	—	—	2.0 ^{+1.1}	—	—	—	1.05 ^{+0.14}	—
Ross 128 HARPS+Carmenes	IP _{circ} + GP-QP	2.2 ^{+0.6}	-4.5 ^{+1.6}	2.2 ^{+1.2}	-0.0 ^{+0.6}	0.64 ^{+0.17}	0.5 ^{+0.4}	1.08 ^{+0.13}	1.4 ^{+0.3}
GJ 832 HARPS	2P _{ecc} + GP-SHO	4.3 ^{+0.3}	7.7 ^{+1.4}	—	—	0.55 ^{+0.32}	0.44 ^{+0.18}	—	—
GJ 674 HARPS	2P _{ecc} + GP-SHO	6.82 ^{+0.33}	8.96 ^{+0.88}	—	—	5.86 ^{+0.33}	7.72 ^{+0.22}	—	—
Ross 128 HARPS	2P _{ecc} + GP-SHO	1.42 ^{+0.16}	0.36 ^{+0.89}	-0.4 ^{+0.4}	—	1.11 ^{+0.20}	0.52 ^{+0.18}	1.27 ^{+0.04}	—
Ross 128 RedDots	2P _{ecc} + GP-SHO	—	—	1.3 ^{+0.9}	—	—	—	0.66 ^{+0.26}	—
Ross 128 HARPS+Carmenes	2P _{ecc} + GP-SHO	2.3 ^{+0.6}	-2.9 ^{+0.7}	2.3 ^{+0.5}	0.2 ^{+0.9}	0.29 ^{+0.21}	0.6 ^{+0.8}	0.94 ^{+0.16}	2.1 ^{+0.4}
GJ 832 HARPS	2P _{circ} + GP-SHO	4.4 ^{+0.3}	7.8 ^{+1.4}	—	—	0.57 ^{+0.29}	0.27 ^{+0.19}	—	—
GJ 674 HARPS	2P _{circ} + GP-SHO	5.7 ^{+0.3}	9.82 ^{+0.13}	—	—	1.69 ^{+0.17}	1.8 ^{+0.3}	—	—
Ross 128 HARPS	2P _{circ} + GP-SHO	2.0 ^{+0.3}	-5.0 ^{+0.8}	1.0 ^{+1.4}	—	0.44 ^{+0.05}	0.22 ^{+0.27}	0.65 ^{+0.14}	—
Ross 128 RedDots	2P _{circ} + GP-SHO	—	—	2.2 ^{+1.3}	—	—	—	0.5 ^{+0.3}	—
Ross 128 HARPS+Carmenes	2P _{circ} + GP-SHO	1.3 ^{+0.6}	-4.75 ^{+1.23}	1.34 ^{+0.81}	-0.02 ^{+0.09}	0.139 ^{+0.162}	0.11 ^{+0.34}	0.66 ^{+0.03}	1.69 ^{+0.09}
GJ 832 HARPS	2P _{ecc} + GP-dSHO	3.8 ^{+0.6}	8.6 ^{+0.9}	—	—	0.73 ^{+0.26}	0.56 ^{+0.15}	—	—

Table G.6. continued.

		$\mu_{\text{H-pre}}$	$\mu_{\text{H-post}}$	$\mu_{\text{H-warmup}}$	μ_{Carmenes}	$\sigma_{\text{H-pre}}$	$\sigma_{\text{H-post}}$	$\sigma_{\text{H-warmup}}$	σ_{Carmenes}
GJ 674 HARPS	2P _{ecc} + GP-dSHO	6.947 ^{+0.036} _{-0.021}	8.61 ^{+0.08} _{-0.04}	—	—	6.125 ^{+0.014} _{-0.023}	11.21 ^{+0.06} _{-0.03}	—	—
Ross 128 HARPS	2P _{ecc} + GP-dSHO	2.2 ^{+0.6} _{-0.4}	-2.3 ^{+0.8} _{-3.8}	5 ⁺³	—	1.07 ^{+0.30} _{-0.04}	1.2 ^{+1.1} _{-0.5}	0.6 ^{+0.4} _{-0.4}	—
Ross 128 RedDots	2P _{ecc} + GP-dSHO	—	—	1.98 ^{+0.21} _{-0.34}	—	—	—	1.13 ^{+0.10} _{-0.03}	—
Ross 128 HARPS+Carmenes	2P _{ecc} + GP-dSHO	1.64 ^{+0.10} _{-0.05}	-1.6 ^{+0.5} _{-0.3}	6.25 ^{+0.25} _{-0.28}	-0.42 ^{+0.14} _{-0.14}	1.162 ^{+0.063} _{-0.021}	1.33 ^{+0.11} _{-0.12}	1.30 ^{+0.05} _{-0.05}	2.32 ^{+0.16} _{-0.27}
GJ 832 HARPS	2P _{circ} + GP-dSHO	4.4 ^{+0.5} _{-0.5}	7.9 ^{+1.2} _{-0.4}	—	—	0.66 ^{+0.15} _{-0.15}	0.39 ^{+0.18} _{-0.20}	—	—
GJ 674 HARPS	2P _{circ} + GP-dSHO	5.99 ^{+0.25} _{-0.21}	9.81 ^{+0.14} _{-0.26}	—	—	1.74 ^{+0.08} _{-0.08}	1.6 ^{+0.3} _{-0.17}	—	—
Ross 128 HARPS	2P _{circ} + GP-dSHO	2.26 ^{+0.24} _{-0.71}	-7.0 ^{+0.8} _{-0.7}	8.8 ^{+0.5} _{-0.48}	—	0.23 ^{+0.78} _{-0.14}	2.21 ^{+0.17} _{-2.04}	1.26 ^{+0.07} _{-0.12}	—
Ross 128 RedDots	2P _{circ} + GP-dSHO	—	—	2.08 ^{+0.34} _{-0.34}	—	—	—	1.04 ^{+0.05} _{-0.05}	—
Ross 128 HARPS+Carmenes	2P _{circ} + GP-dSHO	0.64 ^{+0.07} _{-0.48}	6.50 ^{+0.17} _{-0.97}	4.2 ^{+0.4} _{-0.4}	1.49 ^{+0.07} _{-0.48}	0.830 ^{+0.020} _{-0.020}	1.18 ^{+0.07} _{-0.31}	1.376 ^{+0.018} _{-0.017}	2.52 ^{+0.08} _{-0.05}
GJ 832 HARPS	2P _{ecc} + GP-QP	4.3 ^{+0.4} _{-0.4}	7.9 ^{+1.4} _{-1.6}	—	—	0.72 ^{+0.14} _{-0.14}	0.53 ^{+0.16} _{-0.16}	—	—
GJ 674 HARPS	2P _{ecc} + GP-QP	6.0 ^{+0.3} _{-0.4}	-1.6 ^{+0.5} _{-0.4}	—	—	2.92 ^{+0.04} _{-0.04}	2.93 ^{+0.10} _{-0.13}	—	—
Ross 128 HARPS	2P _{ecc} + GP-QP	-8.9 ^{+1.2} _{-0.7}	3 ⁺⁴ ₋₄	-2 ⁺⁴	—	1.35 ^{+0.11} _{-0.09}	0.9 ^{+0.7} _{-0.6}	1.27 ^{+0.09} _{-0.06}	—
Ross 128 RedDots	2P _{ecc} + GP-QP	—	—	2.6 ^{+0.8} _{-0.8}	—	—	—	1.29 ^{+0.06} _{-0.06}	—
Ross 128 HARPS+Carmenes	2P _{ecc} + GP-QP	1.8 ^{+2.0} _{-0.3}	-5.2 ^{+1.5} _{-1.6}	0.8 ^{+1.9} _{-1.5}	4.4 ^{+1.7} _{-1.5}	1.60 ^{+0.13} _{-0.14}	1.6 ^{+0.4} _{-0.4}	1.39 ^{+0.10} _{-0.07}	1.42 ^{+0.25} _{-0.22}
GJ 832 HARPS	2P _{circ} + GP-QP	4.5 ^{+0.3} _{-0.4}	7.6 ^{+1.7} _{-1.6}	—	—	0.67 ^{+0.18} _{-0.18}	0.33 ^{+0.18} _{-0.18}	—	—
GJ 674 HARPS	2P _{circ} + GP-QP	-1.3 ^{+0.4} _{-0.3}	-3.93 ^{+0.46} _{-0.72}	—	—	2.090 ^{+0.022} _{-0.022}	2.05 ^{+0.05} _{-0.05}	—	—
Ross 128 HARPS	2P _{circ} + GP-QP	2.9 ^{+0.7} _{-4.7}	-2.4 ^{+7.7} _{-1.3}	2.9 ^{+1.5} _{-0.5}	—	1.27 ^{+0.20} _{-0.36}	1.3 ^{+1.5} _{-0.7}	1.52 ^{+0.36} _{-0.18}	—
Ross 128 RedDots	2P _{circ} + GP-QP	—	—	4.6 ^{+0.5} _{-0.5}	—	—	—	1.14 ^{+0.11} _{-0.11}	—
Ross 128 HARPS+Carmenes	2P _{circ} + GP-QP	2.38 ^{+0.22} _{-0.09}	-4.56 ^{+0.91} _{-0.11}	-0.95 ^{+3.76} _{-0.17}	0.10 ^{+0.19} _{-0.09}	0.408 ^{+0.108} _{-0.016}	1.22 ^{+0.04} _{-0.78}	0.855 ^{+0.137} _{-0.021}	1.19 ^{+0.11} _{-0.04}

Table G.7. Bayesian posteriors for the general GP parameters obtained during the model comparison.

	S_0	Q	ω_0	Q_0	f	dQ	P_{GP}	α
GJ 832 HARPS	OP	—	—	—	—	—	—	—
GJ 674 HARPS	OP	—	—	—	—	—	—	—
Ross 128 HARPS	OP	—	—	—	—	—	—	—
Ross 128 RedDots	OP	—	—	—	—	—	—	—
Ross 128 HARPS+Carmenes	OP	—	—	—	—	—	—	—
GJ 832 HARPS	IP _{ecc}	—	—	—	—	—	—	—
GJ 674 HARPS	IP _{ecc}	—	—	—	—	—	—	—
Ross 128 HARPS	IP _{ecc}	—	—	—	—	—	—	—
Ross 128 RedDots	IP _{ecc}	—	—	—	—	—	—	—
Ross 128 HARPS+Carmenes	IP _{ecc}	—	—	—	—	—	—	—
GJ 832 HARPS	IP _{circ}	—	—	—	—	—	—	—
GJ 674 HARPS	IP _{circ}	—	—	—	—	—	—	—
Ross 128 HARPS	IP _{circ}	—	—	—	—	—	—	—
Ross 128 RedDots	IP _{circ}	—	—	—	—	—	—	—
Ross 128 HARPS+Carmenes	IP _{circ}	—	—	—	—	—	—	—
GJ 832 HARPS	2P _{ecc}	—	—	—	—	—	—	—
GJ 674 HARPS	2P _{ecc}	—	—	—	—	—	—	—
Ross 128 HARPS	2P _{ecc}	—	—	—	—	—	—	—
Ross 128 RedDots	2P _{ecc}	—	—	—	—	—	—	—
Ross 128 HARPS+Carmenes	2P _{ecc}	—	—	—	—	—	—	—
GJ 832 HARPS	2P _{circ}	—	—	—	—	—	—	—
GJ 674 HARPS	2P _{circ}	—	—	—	—	—	—	—
Ross 128 HARPS	2P _{circ}	—	—	—	—	—	—	—
Ross 128 RedDots	2P _{circ}	—	—	—	—	—	—	—
Ross 128 HARPS+Carmenes	2P _{circ}	—	—	—	—	—	—	—
GJ 832 HARPS	OP + GP-SHO	107 ⁺⁶⁴ ₋₆₇	1172 ⁺²⁷⁷⁵ ₋₇₁₄	0.00171 ^{+0.00004} _{-0.00004}	0.14 ^{+0.08} _{-0.03}	0.40 ^{+0.35} _{-0.23}	0.27 ^{+0.49} _{-0.13}	0.0000023 ^{+0.0000009} _{-0.0000007}
GJ 674 HARPS	OP + GP-SHO	45 ⁺⁹ ₋₈	1.47 ^{+0.27} _{-0.23}	0.995 ^{+0.008} _{-0.008}	20274 ⁺⁵¹⁷²⁷ ₋₂₀₂₇₃	0.16 ^{+0.27} _{-0.19}	8410 ⁺⁵⁰⁸⁹⁹ ₋₈₄₀₇	0.000000016 ^{+0.000000007} _{-0.000000006}
Ross 128 HARPS	OP + GP-SHO	54 ⁺³⁷ ₋₂₀	0.15 ^{+0.06} _{-0.05}	0.82 ^{+0.13} _{-0.17}	0.13 ^{+0.06} _{-0.03}	0.73 ^{+0.15} _{-0.27}	0.15 ^{+0.15} _{-0.04}	0.0054 ^{+0.0030} _{-0.0016}
Ross 128 RedDots	OP + GP-SHO	95 ⁺⁶⁴ ₋₅₄	0.15 ^{+0.08} _{-0.04}	0.84 ^{+0.17} _{-0.17}	0.15 ^{+0.09} _{-0.04}	0.67 ^{+0.23} _{-0.31}	0.24 ^{+757.51} _{-0.1}	0.010 ^{+0.008} _{-0.004}
Ross 128 HARPS+Carmenes	OP + GP-SHO	46 ⁺²⁵ ₋₁₅	0.16 ^{+0.06} _{-0.04}	0.84 ^{+0.17} _{-0.16}	0.132 ^{+0.061} _{-0.025}	0.73 ^{+0.19} _{-0.28}	0.15 ^{+0.10} _{-0.04}	0.0049 ^{+0.0019} _{-0.0012}
GJ 832 HARPS	OP + GP-dHO	—	—	—	—	—	—	—
GJ 674 HARPS	OP + GP-dHO	—	—	—	—	—	—	—
Ross 128 HARPS	OP + GP-dHO	—	—	—	—	—	—	—
Ross 128 RedDots	OP + GP-dHO	—	—	—	—	—	—	—
Ross 128 HARPS+Carmenes	OP + GP-dHO	—	—	—	—	—	—	—
GJ 832 HARPS	OP + GP-QP	—	—	—	—	—	—	—
GJ 674 HARPS	OP + GP-QP	—	—	—	—	—	—	—
Ross 128 HARPS	OP + GP-QP	—	—	—	—	—	—	—
Ross 128 RedDots	OP + GP-QP	—	—	—	—	—	—	—
Ross 128 HARPS+Carmenes	OP + GP-QP	—	—	—	—	—	—	—
GJ 832 HARPS	IP _{ecc} + GP-SHO	24 ⁺¹⁷ ₋₉	0.5 ^{+0.3} _{-0.3}	0.32 ^{+0.29} _{-0.07}	—	—	—	—
GJ 674 HARPS	IP _{ecc} + GP-SHO	90 ⁺⁴⁴ ₋₂₈	0.38 ^{+0.16} _{-0.14}	0.31 ^{+0.09} _{-0.05}	—	—	—	—

Table G.7. continued.

		S_0	Q	ω_0	Q_0	f	dQ	P_{CP}	α
Ross 128 HARPS	IP _{ecc} + GP-SHO	127 ⁺⁵⁶	0.09 ^{+0.05}	0.7 ^{+0.3}	—	—	—	—	—
Ross 128 RedDots	IP _{ecc} + GP-SHO	78 ⁺⁶⁹	0.12 ^{+0.06}	0.81 ^{+0.13}	—	—	—	—	—
Ross 128 HARPS+Carmenes	IP _{ecc} + GP-SHO	103 ⁺⁵²	0.068 ^{+0.040}	0.70 ^{+0.17}	—	—	—	—	—
GJ 832 HARPS	IP _{circ} + GP-SHO	23 ⁺³⁸	0.5 ^{+0.3}	0.32 ^{+0.28}	—	—	—	—	—
GJ 674 HARPS	IP _{circ} + GP-SHO	83 ⁺⁴⁹	0.31 ^{+0.37}	0.35 ^{+0.37}	—	—	—	—	—
Ross 128 HARPS	IP _{circ} + GP-SHO	126 ⁺³⁸	0.064 ^{+0.039}	0.70 ^{+0.17}	—	—	—	—	—
Ross 128 RedDots	IP _{circ} + GP-SHO	113 ⁺⁴⁷	0.10 ^{+0.06}	0.80 ^{+0.14}	—	—	—	—	—
Ross 128 HARPS+Carmenes	IP _{circ} + GP-SHO	102 ⁺³⁶	0.08 ^{+0.05}	0.65 ^{+0.23}	—	—	—	—	—
GJ 832 HARPS	IP _{ecc} + GP-dSHO	—	—	0.33 ^{+0.65}	0.66 ^{+0.24}	2.1 ^{+479.3}	37 ⁺⁴	0.030 ^{+0.025}	—
GJ 674 HARPS	IP _{ecc} + GP-dSHO	—	—	0.17 ^{+0.14}	0.74 ^{+0.18}	158 ⁺²⁰⁶⁶⁷	36.7 ^{+1.8}	0.00029 ^{+0.00015}	—
Ross 128 HARPS	IP _{ecc} + GP-dSHO	—	—	0.41 ^{+0.38}	0.6 ^{+0.3}	6 ⁺³¹⁷²	119 ⁺²	0.0003 ^{+0.0025}	—
Ross 128 RedDots	IP _{ecc} + GP-dSHO	—	—	1.9 ^{+27.7}	0.74 ^{+0.18}	99 ⁺⁵⁰⁷⁹	141 ⁺³⁸	0.00023 ^{+0.00863}	—
Ross 128 HARPS+Carmenes	IP _{ecc} + GP-dSHO	—	—	0.7 ^{+1.4}	0.5 ^{+0.3}	1279 ⁺²³⁶³⁴	132.1 ^{+2.1}	0.00009 ^{+0.00156}	—
Ross 128 HARPS	IP _{circ} + GP-dSHO	—	—	0.39 ^{+0.29}	0.65 ^{+0.25}	2.2 ^{+12.9}	36.5 ^{+3.6}	0.03 ^{+0.03}	—
GJ 832 HARPS	IP _{circ} + GP-dSHO	—	—	0.19 ^{+0.19}	0.73 ^{+0.19}	4155 ⁺³⁴⁶⁴⁹	36.70 ^{+0.05}	0.000000028 ^{+0.0000000018}	—
GJ 674 HARPS	IP _{circ} + GP-dSHO	—	—	0.4 ^{+0.9}	0.6 ^{+0.3}	7 ⁺³⁸⁴⁵	118 ⁺²⁰	0.0007 ^{+0.00007}	—
Ross 128 HARPS	IP _{circ} + GP-dSHO	—	—	3088 ⁺³⁷⁰⁶⁹	0.66 ^{+0.23}	8 ⁺¹⁹⁰	136 ⁺³⁰	0.0000000028 ^{+0.0000000012}	—
Ross 128 RedDots	IP _{circ} + GP-dSHO	—	—	0.7 ^{+1.3}	0.6 ^{+0.3}	373 ⁺¹¹⁵²⁸	132.1 ^{+2.4}	0.0007 ^{+0.0001}	—
Ross 128 HARPS+Carmenes	IP _{circ} + GP-dSHO	—	—	—	0.6 ^{+0.3}	—	—	0.000008 ^{+0.004678}	—
GJ 832 HARPS	IP _{ecc} + GP-QP	—	—	—	—	—	—	0.00005 ^{+0.00142}	—
GJ 674 HARPS	IP _{ecc} + GP-QP	—	—	—	—	—	—	—	—
Ross 128 HARPS	IP _{ecc} + GP-QP	—	—	—	—	—	—	—	—
Ross 128 RedDots	IP _{ecc} + GP-QP	—	—	—	—	—	—	—	—
Ross 128 HARPS+Carmenes	IP _{ecc} + GP-QP	—	—	—	—	—	—	—	—
GJ 832 HARPS	2P _{ecc} + GP-SHO	21 ⁺²⁰	0.6 ^{+0.3}	0.30 ^{+0.35}	—	—	—	—	—
GJ 674 HARPS	2P _{ecc} + GP-SHO	124 ⁺⁷	0.00005 ^{+0.00009}	0.65 ^{+0.08}	—	—	—	—	—
Ross 128 HARPS	2P _{ecc} + GP-SHO	164 ⁺⁷	0.60 ^{+0.00004}	0.083 ^{+0.011}	—	—	—	—	—
Ross 128 RedDots	2P _{ecc} + GP-SHO	131 ⁺²⁷	0.08 ^{+0.03}	0.85 ^{+0.109}	—	—	—	—	—
Ross 128 HARPS+Carmenes	2P _{ecc} + GP-SHO	47 ⁺⁴⁷	0.28 ^{+0.33}	0.30 ^{+0.34}	—	—	—	—	—
GJ 832 HARPS	2P _{circ} + GP-SHO	23 ⁺¹⁸	0.5 ^{+0.3}	0.32 ^{+0.21}	—	—	—	—	—
GJ 674 HARPS	2P _{circ} + GP-SHO	105 ⁺⁵⁵	0.14 ^{+0.15}	0.45 ^{+0.37}	—	—	—	—	—
Ross 128 HARPS	2P _{circ} + GP-SHO	129 ⁺⁴⁵	0.057 ^{+0.035}	0.82 ^{+0.20}	—	—	—	—	—
Ross 128 RedDots	2P _{circ} + GP-SHO	152 ⁺²⁸	0.12 ^{+0.08}	0.77 ^{+0.19}	—	—	—	—	—
Ross 128 HARPS+Carmenes	2P _{circ} + GP-SHO	179 ⁺⁸³	0.0665 ^{+0.0022}	0.51 ^{+0.34}	—	—	—	—	—
GJ 832 HARPS	2P _{ecc} + GP-dSHO	—	—	1.3 ^{+3.0}	0.75 ^{+0.13}	27 ⁺¹²³⁹	63 ⁺¹⁰	0.0000000028 ^{+0.0000000018}	—
GJ 674 HARPS	2P _{ecc} + GP-dSHO	—	—	0.1 ^{+0.8}	—	—	—	—	—
Ross 128 HARPS	2P _{ecc} + GP-dSHO	—	—	1.4 ^{+38.0}	0.72 ^{+0.17}	11 ⁺⁴⁵⁰	112 ⁺³¹	0.000008 ^{+0.004678}	—
Ross 128 HARPS	2P _{ecc} + GP-dSHO	—	—	—	—	—	—	—	—

Table G.7. continued.

		S_0	Q	ω_0	Q_0	f	dQ	P_{CP}	α
Ross 128 RedDots	2P _{ecc} + GP-dSHO	-	-	-	242 ⁺⁶³⁶ ₋₂₃₇	0.14 ^{+0.07} _{-0.08}	24 ⁺²³ ₋₁₆	117 ⁺⁷ ₋₁	-
Ross 128 HARPS+Carmentis	2P _{ecc} + GP-dSHO	-	-	-	-1 ⁺⁰	-1 ⁺⁰	-1 ⁺⁰	-1 ⁺⁰	-
GJ 832 HARPS	2P _{circ} + GP-dSHO	-	-	-	0.6 ^{+0.7}	0.68 ^{+0.21}	1.1 ^{+8.6}	36 ⁺³	-
GJ 674 HARPS	2P _{circ} + GP-dSHO	-	-	-	0.23 ^{+0.18} _{-0.14}	0.50 ^{+0.34} _{-0.34}	49 ^{+39.4} ₋₄₈	36.7 ^{+1.7} _{-0.4}	-
Ross 128 HARPS	2P _{circ} + GP-dSHO	-	-	-	0.24 ^{+0.38} _{-0.16}	0.33 ^{+0.03} _{-0.03}	0.16 ^{+0.11}	172 ⁺⁸	-
Ross 128 RedDots	2P _{circ} + GP-dSHO	-	-	-	1260 ⁺⁸¹⁰ ₋₁₄₅	0.27 ^{+0.23} _{-0.06}	44 ⁺³³⁸ ₋₃₁	99 ⁺²⁶	-
Ross 128 HARPS+Carmentis	2P _{circ} + GP-dSHO	-	-	-	0.141 ^{+0.145} _{-0.010}	0.46 ^{+0.06} _{-0.03}	7240 ⁺³⁸⁷ ₋₆₁₃₀	188.3 ^{+1.1} _{-1.3}	-
GJ 832 HARPS	2P _{ecc} + GP-QP	-	-	-	-	-	-	-	0.009 ^{+0.028} _{-0.008}
GJ 674 HARPS	2P _{ecc} + GP-QP	-	-	-	-	-	-	-	-1 ⁺⁰
Ross 128 HARPS	2P _{ecc} + GP-QP	-	-	-	-	-	-	-	0.0000014 ^{+0.0000027} _{-0.0000011}
Ross 128 RedDots	2P _{ecc} + GP-QP	-	-	-	-	-	-	-	0.0000022 ^{+0.0000011} _{-0.0000010}
Ross 128 HARPS+Carmentis	2P _{ecc} + GP-QP	-	-	-	-	-	-	-	0.00000005 ^{+0.0000005} _{-0.0000005}
GJ 832 HARPS	2P _{circ} + GP-QP	-	-	-	-	-	-	-	0.03 ^{+0.03} _{-0.03}
GJ 674 HARPS	2P _{circ} + GP-QP	-	-	-	-	-	-	-	0.000000013 ^{+0.000000004} _{-0.000000004}
Ross 128 HARPS	2P _{circ} + GP-QP	-	-	-	-	-	-	-	0.000008 ^{+0.000008} _{-0.000008}
Ross 128 RedDots	2P _{circ} + GP-QP	-	-	-	-	-	-	-	0.000000008 ^{+0.000000349} _{-0.000000001}
Ross 128 HARPS+Carmentis	2P _{circ} + GP-QP	-	-	-	-	-	-	-	0.000012 ^{+0.000001} _{-0.000006}

Table G.8. Bayesian posteriors for the seasonal GP parameters obtained during the model comparison.

		$\sigma_{\text{dSHO,H-pre}}$	$\sigma_{\text{dSHO,H-post}}$	$\sigma_{\text{dSHO,H-warmup}}$	$\sigma_{\text{dSHO,carmenes}}$	$\sigma_{\text{QP,H-pre}}$	$\sigma_{\text{QP,H-post}}$	$\sigma_{\text{QP,H-warmup}}$	$\sigma_{\text{QP,carmenes}}$
GJ 832 HARPS	0P	—	—	—	—	—	—	—	—
GJ 674 HARPS	0P	—	—	—	—	—	—	—	—
Ross 128 HARPS	0P	—	—	—	—	—	—	—	—
Ross 128 RedDots	0P	—	—	—	—	—	—	—	—
Ross 128 HARPS+Carmenes	0P	—	—	—	—	—	—	—	—
GJ 832 HARPS	1P _{ecc}	—	—	—	—	—	—	—	—
GJ 674 HARPS	1P _{ecc}	—	—	—	—	—	—	—	—
Ross 128 HARPS	1P _{ecc}	—	—	—	—	—	—	—	—
Ross 128 RedDots	1P _{ecc}	—	—	—	—	—	—	—	—
Ross 128 HARPS+Carmenes	1P _{ecc}	—	—	—	—	—	—	—	—
GJ 832 HARPS	1P _{circ}	—	—	—	—	—	—	—	—
GJ 674 HARPS	1P _{circ}	—	—	—	—	—	—	—	—
Ross 128 HARPS	1P _{circ}	—	—	—	—	—	—	—	—
Ross 128 RedDots	1P _{circ}	—	—	—	—	—	—	—	—
Ross 128 HARPS+Carmenes	1P _{circ}	—	—	—	—	—	—	—	—
GJ 832 HARPS	2P _{ecc}	—	—	—	—	—	—	—	—
GJ 674 HARPS	2P _{ecc}	—	—	—	—	—	—	—	—
Ross 128 HARPS	2P _{ecc}	—	—	—	—	—	—	—	—
Ross 128 RedDots	2P _{ecc}	—	—	—	—	—	—	—	—
Ross 128 HARPS+Carmenes	2P _{ecc}	—	—	—	—	—	—	—	—
GJ 832 HARPS	2P _{circ}	—	—	—	—	—	—	—	—
GJ 674 HARPS	2P _{circ}	—	—	—	—	—	—	—	—
Ross 128 HARPS	2P _{circ}	—	—	—	—	—	—	—	—
Ross 128 RedDots	2P _{circ}	—	—	—	—	—	—	—	—
Ross 128 HARPS+Carmenes	2P _{circ}	—	—	—	—	—	—	—	—
GJ 832 HARPS	0P + GP-SHO	—	—	—	—	—	—	—	—
GJ 674 HARPS	0P + GP-SHO	—	—	—	—	—	—	—	—
Ross 128 HARPS	0P + GP-SHO	—	—	—	—	—	—	—	—
Ross 128 RedDots	0P + GP-SHO	—	—	—	—	—	—	—	—
Ross 128 HARPS+Carmenes	0P + GP-SHO	—	—	—	—	—	—	—	—
GJ 832 HARPS	0P + GP-dHO	10.8 ^{+1.7} _{-1.3}	10.8 ^{+2.5} _{-1.9}	—	—	—	—	—	—
GJ 674 HARPS	0P + GP-dHO	5.5 ^{+2.0} _{-1.2}	7.3 ^{+2.7} _{-2.0}	—	—	—	—	—	—
Ross 128 HARPS	0P + GP-dHO	2.20 ^{+0.32} _{-0.25}	2.7 ^{+0.9} _{-0.5}	2.9 ^{+0.7} _{-0.5}	—	—	—	—	—
Ross 128 RedDots	0P + GP-dHO	—	—	2.6 ^{+1.1} _{-0.4}	—	—	—	—	—
Ross 128 HARPS+Carmenes	0P + GP-dHO	2.16 ^{+0.27} _{-0.24}	2.7 ^{+0.6} _{-0.5}	2.9 ^{+0.8} _{-0.5}	1.9 ^{+0.5} _{-0.5}	—	—	—	—
GJ 832 HARPS	0P + GP-QP	—	—	—	—	9.8 ^{+2.9} _{-1.9}	19 ⁺¹⁰ ₋₆	—	—
GJ 674 HARPS	0P + GP-QP	—	—	—	—	17 ⁺¹¹ ₋₇	19 ⁺¹³ ₋₇	—	—
Ross 128 HARPS	0P + GP-QP	—	—	—	—	2.2 ^{+0.3} _{-0.3}	2.9 ^{+0.8} _{-0.6}	2.4 ^{+0.7} _{-0.5}	—
Ross 128 RedDots	0P + GP-QP	—	—	—	—	—	—	2.1 ^{+0.3} _{-0.3}	—
Ross 128 HARPS+Carmenes	0P + GP-QP	—	—	—	—	—	—	2.4 ^{+0.7} _{-0.5}	2.0 ^{+0.5} _{-0.4}
GJ 832 HARPS	1P _{ecc} + GP-SHO	—	—	—	—	—	—	—	—
GJ 674 HARPS	1P _{ecc} + GP-SHO	—	—	—	—	—	—	—	—
Ross 128 HARPS	1P _{ecc} + GP-SHO	—	—	—	—	—	—	—	—

Table G.8. continued.

		$\sigma_{\text{dSHO,H-pre}}$	$\sigma_{\text{dSHO,H-post}}$	$\sigma_{\text{dSHO,H-warmup}}$	$\sigma_{\text{dSHO,carmenes}}$	$\sigma_{\text{QP,H-pre}}$	$\sigma_{\text{QP,H-post}}$	$\sigma_{\text{QP,H-warmup}}$	$\sigma_{\text{QP,carmenes}}$
Ross 128 RedDots	IP _{ecc} + GP-SHO	—	—	—	—	—	—	—	—
Ross 128 HARPS+Carmenes	IP _{ecc} + GP-SHO	—	—	—	—	—	—	—	—
GJ 832 HARPS	IP _{circ} + GP-SHO	—	—	—	—	—	—	—	—
GJ 674 HARPS	IP _{circ} + GP-SHO	—	—	—	—	—	—	—	—
Ross 128 HARPS	IP _{circ} + GP-SHO	—	—	—	—	—	—	—	—
Ross 128 RedDots	IP _{circ} + GP-SHO	—	—	—	—	—	—	—	—
Ross 128 HARPS+Carmenes	IP _{circ} + GP-SHO	—	—	—	—	—	—	—	—
GJ 832 HARPS	IP _{ecc} + GP-dSHO	1.8 ^{+0.5} _{-0.3}	2.1 ^{+0.5} _{-0.4}	—	—	—	—	—	—
GJ 674 HARPS	IP _{ecc} + GP-dSHO	3.2 ^{+0.6} _{-0.4}	5.0 ^{+0.7} _{-0.7}	—	—	—	—	—	—
Ross 128 HARPS	IP _{ecc} + GP-dSHO	2.4 ^{+0.7} _{-0.5}	3.8 ^{+0.7} _{-1.1}	1.97 ^{+0.98} _{-0.59}	—	—	—	—	—
Ross 128 RedDots	IP _{ecc} + GP-dSHO	—	—	2.4 ^{+0.8} _{-0.8}	—	—	—	—	—
Ross 128 HARPS+Carmenes	IP _{ecc} + GP-dSHO	2.9 ^{+1.1} _{-0.6}	4.7 ^{+2.5} _{-1.5}	2.2 ^{+0.8} _{-0.7}	1.8 ^{+0.7} _{-0.5}	—	—	—	—
GJ 832 HARPS	IP _{circ} + GP-dSHO	1.8 ^{+0.4} _{-0.3}	2.1 ^{+0.5} _{-0.4}	—	—	—	—	—	—
GJ 674 HARPS	IP _{circ} + GP-dSHO	2.8 ^{+0.6} _{-0.4}	5.6 ^{+0.7} _{-0.7}	—	—	—	—	—	—
Ross 128 HARPS	IP _{circ} + GP-dSHO	2.3 ^{+0.8} _{-0.5}	3.8 ^{+0.7} _{-1.1}	1.96 ^{+1.00} _{-0.58}	—	—	—	—	—
Ross 128 RedDots	IP _{circ} + GP-dSHO	—	—	2.2 ^{+0.7} _{-0.7}	—	—	—	—	—
Ross 128 HARPS+Carmenes	IP _{circ} + GP-dSHO	2.6 ^{+0.7} _{-0.5}	4.3 ^{+2.3} _{-1.4}	2.1 ^{+0.7} _{-0.7}	1.7 ^{+0.6} _{-0.4}	—	—	—	—
GJ 832 HARPS	IP _{ecc} + GP-QP	—	—	—	—	—	—	—	—
GJ 674 HARPS	IP _{ecc} + GP-QP	—	—	—	—	—	—	—	—
Ross 128 HARPS	IP _{ecc} + GP-QP	—	—	—	—	—	—	—	—
Ross 128 RedDots	IP _{ecc} + GP-QP	—	—	—	—	—	—	—	—
Ross 128 HARPS+Carmenes	IP _{ecc} + GP-QP	—	—	—	—	—	—	—	—
GJ 832 HARPS	IP _{circ} + GP-QP	—	—	—	—	—	—	—	—
GJ 674 HARPS	IP _{circ} + GP-QP	—	—	—	—	—	—	—	—
Ross 128 HARPS	IP _{circ} + GP-QP	—	—	—	—	—	—	—	—
Ross 128 RedDots	IP _{circ} + GP-QP	—	—	—	—	—	—	—	—
Ross 128 HARPS+Carmenes	IP _{circ} + GP-QP	—	—	—	—	—	—	—	—
GJ 832 HARPS	2P _{ecc} + GP-SHO	—	—	—	—	—	—	—	—
GJ 674 HARPS	2P _{ecc} + GP-SHO	—	—	—	—	—	—	—	—
Ross 128 HARPS	2P _{ecc} + GP-SHO	—	—	—	—	—	—	—	—
Ross 128 RedDots	2P _{ecc} + GP-SHO	—	—	—	—	—	—	—	—
Ross 128 HARPS+Carmenes	2P _{ecc} + GP-SHO	—	—	—	—	—	—	—	—
GJ 832 HARPS	2P _{circ} + GP-SHO	—	—	—	—	—	—	—	—
GJ 674 HARPS	2P _{circ} + GP-SHO	—	—	—	—	—	—	—	—
Ross 128 HARPS	2P _{circ} + GP-SHO	—	—	—	—	—	—	—	—
Ross 128 RedDots	2P _{circ} + GP-SHO	—	—	—	—	—	—	—	—
Ross 128 HARPS+Carmenes	2P _{circ} + GP-SHO	—	—	—	—	—	—	—	—
GJ 832 HARPS	2P _{ecc} + GP-dSHO	2.12 ^{+0.96} _{-0.49}	2.6 ^{+1.5} _{-0.7}	—	—	—	—	—	—
GJ 674 HARPS	2P _{ecc} + GP-dSHO	-1 ⁺⁰ ₋₀	-1 ⁺⁰ ₋₀	—	—	—	—	—	—
Ross 128 HARPS	2P _{ecc} + GP-dSHO	4.0 ^{+0.4} _{-1.8}	8 ⁺¹⁸ ₋₄	—	—	—	—	—	—
Ross 128 RedDots	2P _{ecc} + GP-dSHO	—	—	54 ⁺¹⁰ ₋₂₈	—	—	—	—	—
Ross 128 HARPS+Carmenes	2P _{ecc} + GP-dSHO	-1 ⁺⁰ ₋₀	-1 ⁺⁰ ₋₀	3.0 ^{+3.7} _{-1.3}	—	—	—	—	—
Ross 128 HARPS+Carmenes	2P _{ecc} + GP-dSHO	-1 ⁺⁰ ₋₀	-1 ⁺⁰ ₋₀	-1 ⁺⁰ ₋₀	-1 ⁺⁰ ₋₀	—	—	—	—

Table G.8. continued.

		$\sigma_{\text{dSHO,H-pre}}$	$\sigma_{\text{dSHO,H-post}}$	$\sigma_{\text{dSHO,H-warmup}}$	$\sigma_{\text{dSHO,carmenes}}$	$\sigma_{\text{QP,H-pre}}$	$\sigma_{\text{QP,H-post}}$	$\sigma_{\text{QP,H-warmup}}$	$\sigma_{\text{QP,carmenes}}$
GJ 832 HARPS	2P _{circ} + GP-dSHO	1.81 ^{+0.28} _{-0.23}	2.0 ^{+0.3} _{-0.1}	—	—	—	—	—	—
GJ 674 HARPS	2P _{circ} + GP-dSHO	2.5 ^{+0.3} _{-0.4}	5.5 ^{+1.1} _{-0.8}	—	—	—	—	—	—
Ross 128 HARPS	2P _{circ} + GP-dSHO	3.5 ^{+0.8} _{-0.9}	27.7 ^{+6.1} _{-2.3}	5.5 ^{+2.8} _{-1.6}	—	—	—	—	—
Ross 128 RedDots	2P _{circ} + GP-dSHO	—	—	3.5 ^{+3.8} _{-1.84}	—	—	—	—	—
Ross 128 HARPS+Carmenes	2P _{circ} + GP-dSHO	3.93 ^{+0.98} _{-0.24}	13.3 ^{+0.7} _{-0.4}	4.61 ^{+1.84} _{-0.23}	6.54 ^{+0.11} _{-0.54}	—	—	—	—
GJ 832 HARPS	2P _{ecc} + GP-QP	—	—	—	—	1.8 ^{+0.3} _{-0.3}	2.0 ^{+0.4} _{-0.3}	—	—
GJ 674 HARPS	2P _{ecc} + GP-QP	—	—	—	—	-1 ⁺⁰ ₋₀	-1 ⁺⁰ ₋₀	—	—
Ross 128 HARPS	2P _{ecc} + GP-QP	—	—	—	—	12 ⁺²¹ ₋₅	28 ⁺⁷ ₋₆	18 ⁺¹⁷ ₋₉	—
Ross 128 RedDots	2P _{ecc} + GP-QP	—	—	—	—	—	—	1.8 ^{+1.0} _{-0.5}	—
Ross 128 HARPS+Carmenes	2P _{ecc} + GP-QP	—	—	—	—	12 ⁺⁷ ₋₇	28 ⁺¹⁴ ₋₁₁	49 ⁺¹⁰ ₋₁₂	92 ⁺⁵ ₋₅
GJ 832 HARPS	2P _{ecc} + GP-QP	—	—	—	—	1.81 ^{+0.24} _{-0.20}	1.9 ^{+0.3} _{-0.3}	—	—
GJ 674 HARPS	2P _{circ} + GP-QP	—	—	—	—	34.1 ^{+0.6} _{-0.4}	16.6 ^{+0.5} _{-0.5}	—	—
Ross 128 HARPS	2P _{circ} + GP-QP	—	—	—	—	2.0 ^{+68.4} _{-0.5}	4.3 ^{+17.1} _{-1.8}	15 ⁺³¹ _{-5.4}	—
Ross 128 RedDots	2P _{circ} + GP-QP	—	—	—	—	—	—	4.4 ^{+5.4} _{-1.7}	—
Ross 128 HARPS+Carmenes	2P _{circ} + GP-QP	—	—	—	—	1.85 ^{+0.22} _{-0.09}	3.25 ^{+0.08} _{-0.49}	7.23 ^{+0.18} _{-0.39}	2.06 ^{+0.05} _{-0.53}

Table G.9. Bayesian posteriors for the parameters of planet 1 obtained during the model comparison.

	K_1	P_1	$\sqrt{e_1} \cos \omega_1$	$\sqrt{e_1} \sin \omega_1$	$t_{0,1}$	e_1	ω_1
GJ 832 HARPS	—	—	—	—	—	—	—
GJ 674 HARPS	—	—	—	—	—	—	—
Ross 128 HARPS	—	—	—	—	—	—	—
Ross 128 RedDots	—	—	—	—	—	—	—
Ross 128 HARPS+Carmenes	—	—	—	—	—	—	—
GJ 832 HARPS	$17.5^{+0.4}_{-0.4}$	3802^{+35}_{-46}	$0.05^{+0.10}_{-0.11}$	$-0.05^{+0.11}_{-0.09}$	2456350^{+34}_{-46}	$0.020^{+0.019}_{-0.014}$	41^{+84}_{-29}
GJ 674 HARPS	$8.9^{+0.3}_{-0.3}$	$4.69507^{+0.00007}_{-0.00007}$	$-0.28^{+0.07}_{-0.06}$	$0.31^{+0.06}_{-0.07}$	$2455253.77^{+6.04}_{-0.04}$	$0.17^{+0.03}_{-0.03}$	132^{+11}_{-11}
Ross 128 HARPS	$1.53^{+0.20}_{-0.19}$	$9.8555^{+0.0015}_{-0.0015}$	$0.25^{+0.20}_{-0.30}$	$0.06^{+0.23}_{-0.24}$	$2459203.9^{+0.5}_{-0.5}$	$0.13^{+0.14}_{-0.09}$	39^{+57}_{-26}
Ross 128 RedDots	$1.8^{+1.6}_{-0.6}$	$9.91^{+0.05}_{-0.13}$	$0.2^{+0.3}_{-0.4}$	$0.6^{+0.3}_{-0.5}$	$2459204.2^{+0.1}_{-0.1}$	$0.6^{+0.3}_{-0.4}$	73^{+26}_{-34}
Ross 128 HARPS+Carmenes	$1.55^{+0.18}_{-0.17}$	$9.8556^{+0.0014}_{-0.0015}$	$0.14^{+0.22}_{-0.27}$	$0.05^{+0.22}_{-0.23}$	$2459213.9^{+0.4}_{-0.4}$	$0.10^{+0.10}_{-0.07}$	52^{+70}_{-36}
GJ 832 HARPS	$17.6^{+0.3}_{-0.3}$	3797^{+41}_{-41}	—	—	2456364^{+17}_{-21}	—	—
GJ 674 HARPS	$8.6^{+0.3}_{-0.3}$	$4.69502^{+0.00008}_{-0.00008}$	—	—	$2455272.41^{+0.03}_{-0.03}$	—	—
Ross 128 HARPS	$1.51^{+0.18}_{-0.18}$	$9.8558^{+0.0013}_{-0.0013}$	—	—	$2459214.1^{+0.3}_{-0.4}$	—	—
Ross 128 RedDots	$1.3^{+0.3}_{-0.3}$	$9.84^{+0.12}_{-0.10}$	—	—	$2459205.4^{+8.7}_{-8.8}$	—	—
Ross 128 HARPS+Carmenes	$1.54^{+0.17}_{-0.17}$	$9.8558^{+0.0013}_{-0.0013}$	—	—	$2459213.8^{+0.4}_{-0.7}$	—	—
GJ 832 HARPS	$1.3^{+0.3}_{-0.7}$	351^{+396}_{-314}	$0.61^{+0.08}_{-0.40}$	$-0.31^{+0.18}_{-0.36}$	2455620^{+214}_{-62}	$0.51^{+0.33}_{-0.21}$	47^{+30}_{-37}
GJ 674 HARPS	$8.58^{+0.23}_{-0.23}$	$4.69509^{+0.00006}_{-0.00006}$	$-0.29^{+0.05}_{-0.05}$	$0.30^{+0.05}_{-0.05}$	$2455239.68^{+0.03}_{-0.04}$	$0.17^{+0.03}_{-0.03}$	134^{+9}_{-9}
Ross 128 HARPS	$0.66^{+0.03}_{-0.03}$	$5.717^{+0.012}_{-0.051}$	$-0.71^{+0.03}_{-0.09}$	$0.049^{+0.014}_{-0.015}$	$2459100.96^{+0.10}_{-0.11}$	$0.51^{+0.13}_{-0.05}$	$176.1^{+1.2}_{-1.0}$
Ross 128 RedDots	$1.9^{+1.2}_{-0.9}$	$3.7^{+0.7}_{-2.7}$	$0.71^{+0.24}_{-1.03}$	$0.18^{+0.39}_{-0.19}$	$2459103.4^{+0.9}_{-1.6}$	$0.84^{+0.11}_{-0.10}$	38^{+77}_{-37}
Ross 128 HARPS+Carmenes	$0.512^{+0.022}_{-0.025}$	$2.33^{+0.03}_{-0.08}$	$-0.726^{+0.005}_{-0.005}$	$0.099^{+0.017}_{-0.015}$	$2459103.140^{+0.022}_{-0.035}$	$0.538^{+0.008}_{-0.008}$	$172.2^{+1.1}_{-1.3}$
GJ 832 HARPS	$1.38^{+0.19}_{-0.13}$	$36.601^{+0.015}_{-0.015}$	—	—	$2455293.0^{+1.1}_{-1.3}$	—	—
GJ 674 HARPS	$8.4^{+0.3}_{-0.3}$	$4.69505^{+0.00007}_{-0.00007}$	—	—	$2455220.75^{+0.03}_{-0.03}$	—	—
Ross 128 HARPS	$0.13^{+0.14}_{-0.09}$	$5.8^{+0.8}_{-1.4}$	—	—	$2459105.9^{+0.7}_{-1.3}$	—	—
Ross 128 RedDots	$2.15^{+0.21}_{-0.21}$	$1.0085^{+0.0006}_{-0.0007}$	—	—	$2459105.92^{+0.18}_{-0.17}$	—	—
Ross 128 HARPS+Carmenes	$0.76^{+0.04}_{-0.06}$	$6.27^{+0.21}_{-0.05}$	—	—	$2459103.51^{+0.11}_{-0.29}$	—	—
GJ 832 HARPS	—	—	—	—	—	—	—
GJ 674 HARPS	—	—	—	—	—	—	—
Ross 128 HARPS	—	—	—	—	—	—	—
Ross 128 RedDots	—	—	—	—	—	—	—
Ross 128 HARPS+Carmenes	—	—	—	—	—	—	—
GJ 832 HARPS	—	—	—	—	—	—	—
GJ 674 HARPS	—	—	—	—	—	—	—
Ross 128 HARPS	—	—	—	—	—	—	—
Ross 128 RedDots	—	—	—	—	—	—	—
Ross 128 HARPS+Carmenes	—	—	—	—	—	—	—
GJ 832 HARPS	$17.4^{+0.2}_{-0.2}$	3767^{+57}_{-58}	$0.09^{+0.11}_{-0.11}$	$-0.05^{+0.13}_{-0.11}$	2456329^{+50}_{-60}	$0.031^{+0.027}_{-0.021}$	37^{+75}_{-27}
GJ 674 HARPS	$8.70^{+0.12}_{-0.12}$	$4.69502^{+0.00003}_{-0.00003}$	$-0.370^{+0.018}_{-0.017}$	$0.327^{+0.020}_{-0.021}$	$2455211.594^{+0.015}_{-0.015}$	$0.245^{+0.012}_{-0.012}$	139^{+3}_{-3}

Table G.9. continued.

		K_1	P_1	$\sqrt{e_1} \cos \omega_1$	$\sqrt{e_1} \sin \omega_1$	$f_{0,1}$	e_1	ω_1
Ross 128 HARPS	IP _{ecc} + GP-SHO	1.32 ^{+0.16}	9.8560 ^{+0.0013}	0.39 ^{+0.11}	0.02 ^{+0.18}	2459204.1 ^{+9.5}	0.18 ^{+0.10}	20 ⁺¹⁷
Ross 128 RedDots	IP _{ecc} + GP-SHO	1.3 ^{+0.16}	9.92 ^{+0.013}	0.2 ^{+0.3}	0.2 ^{+0.3}	2459212.7 ^{+1.5}	0.31 ^{+0.41}	59 ⁺⁶⁸
Ross 128 HARPS+Carmenes	IP _{ecc} + GP-SHO	1.44 ^{+0.14}	9.8558 ^{+0.0013}	0.36 ^{+0.11}	0.10 ^{+0.16}	2459213.4 ^{+0.5}	0.17 ^{+0.10}	26 ⁺²⁵
GJ 832 HARPS	IP _{circ} + GP-SHO	17.4 ^{+0.5}	3760 ⁺⁵¹	—	—	2456356 ^{+28.6}	—	—
GJ 674 HARPS	IP _{circ} + GP-SHO	8.21 ^{+0.19}	4.69498 ^{+0.00005}	—	—	2455277.106 ^{+0.024}	—	—
Ross 128 HARPS	IP _{circ} + GP-SHO	1.37 ^{+0.15}	9.8559 ^{+0.0005}	—	—	2459204.3 ^{+0.5}	—	—
Ross 128 RedDots	IP _{circ} + GP-SHO	1.3 ^{+0.14}	9.87 ^{+0.014}	—	—	2459213.3 ^{+1.0}	—	—
Ross 128 HARPS+Carmenes	IP _{circ} + GP-SHO	1.37 ^{+0.13}	9.8557 ^{+0.0012}	—	—	2459204.27 ^{+0.36}	—	—
GJ 832 HARPS	IP _{ecc} + GP-dSHO	17.4 ^{+0.5}	3774 ⁺⁵¹	0.05 ^{+0.12}	-0.06 ^{+0.12}	2456341 ⁺⁴⁵	0.024 ^{+0.024}	46 ⁺⁸⁸
GJ 674 HARPS	IP _{ecc} + GP-dSHO	8.68 ^{+0.11}	4.69502 ^{+0.00003}	-0.371 ^{+0.016}	0.319 ^{+0.020}	2455230.371 ^{-0.014}	0.240 ^{+0.012}	139 ⁺³³
Ross 128 HARPS	IP _{ecc} + GP-dSHO	1.40 ^{+0.13}	9.8554 ^{+0.0003}	0.40 ^{+0.10}	0.16 ^{+0.23}	2459213.4 ^{+0.5}	0.21 ^{+0.09}	26 ⁺²¹
Ross 128 RedDots	IP _{ecc} + GP-dSHO	1.42 ^{+0.13}	9.86 ^{+0.011}	0.33 ^{+0.21}	0.15 ^{+0.18}	2459203.7 ^{+0.3}	0.20 ^{+0.19}	40 ⁺⁴⁸
Ross 128 HARPS+Carmenes	IP _{ecc} + GP-dSHO	1.44 ^{+0.12}	9.8555 ^{+0.0010}	0.36 ^{+0.11}	0.15 ^{+0.18}	2459213.5 ^{+0.5}	0.18 ^{+0.15}	28 ⁺²¹
GJ 832 HARPS	IP _{circ} + GP-dSHO	17.5 ^{+0.4}	3763 ⁺⁵²	—	—	2456355 ^{+28.3}	—	—
GJ 674 HARPS	IP _{circ} + GP-dSHO	8.20 ^{+0.18}	4.69498 ^{+0.00005}	—	—	2455201.978 ^{-0.023}	—	—
Ross 128 HARPS	IP _{circ} + GP-dSHO	1.36 ^{+0.13}	9.8555 ^{+0.0005}	—	—	2459213.97 ^{-0.022}	—	—
Ross 128 RedDots	IP _{circ} + GP-dSHO	1.39 ^{+0.19}	9.84 ^{+0.010}	—	—	2459213.9 ^{+0.5}	—	—
Ross 128 HARPS+Carmenes	IP _{circ} + GP-dSHO	1.39 ^{+0.12}	9.8555 ^{+0.0011}	—	—	2459213.99 ^{-0.19}	—	—
GJ 832 HARPS	IP _{ecc} + GP-QP	17.3 ^{+0.5}	3766 ⁺⁵⁷	0.08 ^{+0.12}	-0.04 ^{+0.12}	2456332 ^{+47.18}	—	—
GJ 674 HARPS	IP _{ecc} + GP-QP	8.60 ^{+0.11}	4.69502 ^{+0.00003}	-0.362 ^{+0.020}	0.321 ^{+0.022}	2455206.889 ^{-0.016}	0.027 ^{+0.029}	43 ⁺⁸²
Ross 128 HARPS	IP _{ecc} + GP-QP	1.40 ^{+0.13}	9.8553 ^{+0.0003}	0.41 ^{+0.10}	0.15 ^{+0.23}	2459213.4 ^{+0.5}	0.234 ^{+0.013}	138 ⁺³³
Ross 128 RedDots	IP _{ecc} + GP-QP	1.38 ^{+0.13}	9.87 ^{+0.011}	0.2 ^{+0.3}	0.3 ^{+0.3}	2459204.04 ^{-0.095}	0.21 ^{+0.10}	25 ⁺¹⁹
Ross 128 HARPS+Carmenes	IP _{ecc} + GP-QP	1.40 ^{+0.12}	9.8553 ^{+0.0011}	0.36 ^{+0.11}	0.15 ^{+0.18}	2459213.5 ^{+0.5}	0.25 ^{+0.31}	59 ⁺³⁹
GJ 832 HARPS	IP _{circ} + GP-QP	17.4 ^{+0.5}	3757 ⁺⁵⁴	—	—	2459213.5 ^{+0.5}	0.18 ^{+0.10}	29 ⁺²⁵
GJ 674 HARPS	IP _{circ} + GP-QP	1.0 ^{+0.3}	2.34750 ^{+0.00018}	—	—	2456354 ^{+28.3}	—	—
Ross 128 HARPS	IP _{circ} + GP-QP	1.35 ^{+0.11}	9.8552 ^{+0.0014}	—	—	2455270 ⁺⁷	—	—
Ross 128 RedDots	IP _{circ} + GP-QP	1.36 ^{+0.12}	9.83 ^{+0.0011}	—	—	2459213.93 ^{+0.21}	—	—
Ross 128 HARPS+Carmenes	IP _{circ} + GP-QP	1.36 ^{+0.12}	9.8553 ^{+0.0011}	—	—	2459213.5 ^{+0.5}	—	—
GJ 832 HARPS	2P _{ecc} + GP-SHO	0.9 ^{+0.4}	504 ⁺⁵⁴⁰	0.5 ^{+0.4}	-0.2 ^{+0.6}	2459204.18 ^{+9.59}	—	—
GJ 674 HARPS	2P _{ecc} + GP-SHO	7.4 ^{+0.4}	4.69499 ^{+0.00018}	0.41 ^{+0.03}	-0.05 ^{+0.05}	2455464 ^{+32.0}	0.70 ^{+0.24}	33 ⁺⁸⁹
Ross 128 HARPS	2P _{ecc} + GP-SHO	0.73 ^{+0.49}	6.04 ^{+0.00019}	-0.94 ^{+0.20}	-0.09 ^{+0.08}	2455267.56 ^{+4.69}	0.172 ^{+0.026}	2.1 ^{+2.5}
Ross 128 RedDots	2P _{ecc} + GP-SHO	0.35 ^{+0.30}	3.8 ^{+0.96}	-0.4 ^{+1.3}	-0.35 ^{+0.30}	2459103.9 ^{+0.4}	0.89 ^{+0.08}	176.9 ^{+2.3}
Ross 128 HARPS+Carmenes	2P _{ecc} + GP-SHO	0.6 ^{+0.3}	1.10906 ^{+0.18932}	0.2 ^{+0.3}	-0.1 ^{+0.4}	2459102.1 ^{+3.7}	0.68 ^{+0.19}	5 ^{+5-6.1}
GJ 832 HARPS	2P _{circ} + GP-SHO	0.5 ^{+0.3}	453 ⁺⁴⁰⁷	—	—	2459102.5 ^{+0.6}	0.5 ^{+0.4}	148 ⁺⁸
GJ 674 HARPS	2P _{circ} + GP-SHO	8.20 ^{+0.19}	4.69499 ^{+0.00005}	—	—	2455395 ⁺³⁸²	—	—
Ross 128 HARPS	2P _{circ} + GP-SHO	0.46 ^{+0.10}	4.034 ^{+0.0005}	—	—	2455291.187 ^{+0.023}	—	—
Ross 128 RedDots	2P _{circ} + GP-SHO	0.32 ^{+0.19}	4.2 ^{+1.6}	—	—	2459104.7 ^{+1.2}	—	—
Ross 128 HARPS+Carmenes	2P _{circ} + GP-SHO	0.41 ^{+0.18}	4.0339 ^{+0.0007}	—	—	2459102.5 ^{+2.5}	—	—
GJ 832 HARPS	2P _{ecc} + GP-dSHO	1.8 ^{+1.4}	304 ⁺³⁰⁰	0.83 ^{+0.10}	-0.0 ^{+0.3}	2459100.46 ^{+1.75}	0.82 ^{+0.12}	15 ⁺²⁵
GJ 674 HARPS	2P _{ecc} + GP-dSHO	-1 ⁺⁰	6.192 ^{+0.039}	-0.988 ^{+0.003}	-1 ⁺⁰	2455545 ⁺³²²	—	—
Ross 128 HARPS	2P _{ecc} + GP-dSHO	0.12 ^{+0.44}	3.2 ^{+2.2}	0.38 ^{+0.08}	-0.3 ^{+0.6}	2455226.31 ^{+0.18}	—	—
Ross 128 HARPS	2P _{ecc} + GP-dSHO	0.12 ^{+0.44}	3.2 ^{+2.2}	0.38 ^{+0.08}	-0.3 ^{+0.6}	2459100.9 ^{+1.4}	0.39 ^{+0.27}	39 ⁺³

Table G.9. continued.

		K_1	P_1	$\sqrt{e_1 \cos \omega_1}$	$\sqrt{e_1 \sin \omega_1}$	$f_{0,1}$	e_1	ω_1
Ross 128 RedDots	$2P_{\text{ecc}} + \text{GP-dSHO}$	$0.56^{+0.14}_{-0.31}$	$1.27^{+0.09}_{-0.18,9}$	$-0.67^{+0.32}_{-0.07,5}$	$0.19^{+0.15}_{-0.11}$	$2459105.2^{+0.7}_{-0.8,5}$	$0.54^{+0.22}_{-0.49}$	157^{+13}_{-26}
Ross 128 HARPS+Carmenes	$2P_{\text{ecc}} + \text{GP-dSHO}$	-1^{+0}_{-0}	$2.473^{+0.068}_{-0.068}$	$0.31^{+0.07}_{-0.05}$	-1^{+0}_{-0}	$2459103.37^{+0.25}_{-0.11}$	-1^{+0}_{-0}	-1^{+0}_{-0}
GJ 832 HARPS	$2P_{\text{circ}} + \text{GP-dSHO}$	$0.5^{+0.4}_{-0.13}$	$378^{+4.8}_{-4.8}$	—	—	$2455468^{+3.20}_{-2.70,023}$	—	—
GJ 674 HARPS	$2P_{\text{circ}} + \text{GP-dSHO}$	$8.21^{+0.13}_{-0.12}$	$4.69497^{+0.00003}_{-0.00003}$	—	—	$2455216.060^{+0.217}_{-0.217}$	—	—
Ross 128 HARPS	$2P_{\text{circ}} + \text{GP-dSHO}$	$0.16^{+0.06}_{-0.03}$	$2.56^{+0.25}_{-0.17}$	—	—	$2459101.86^{+0.41}_{-0.22}$	—	—
Ross 128 RedDots	$2P_{\text{circ}} + \text{GP-dSHO}$	$0.44^{+0.16}_{-0.06,7}$	$2.5^{+1.2}_{-0.7}$	—	—	$2459105.3^{+0.3}_{-0.19}$	—	—
Ross 128 HARPS+Carmenes	$2P_{\text{circ}} + \text{GP-dSHO}$	$0.550^{+0.007}_{-0.008}$	$3.480^{+0.006}_{-0.211}$	—	—	$2459104.59^{+0.19}_{-0.09}$	—	—
GJ 832 HARPS	$2P_{\text{ecc}} + \text{GP-QP}$	$1.3^{+0.2}_{-0.9}$	$922^{+4.5}_{-0.70}$	$-0.66^{+0.34}_{-0.21}$	$0.6^{+0.3}_{-0.3}$	$2455680^{+1.31}_{-1.31}$	$0.90^{+0.08}_{-0.20}$	$137^{+22}_{-1.06}$
GJ 674 HARPS	$2P_{\text{ecc}} + \text{GP-QP}$	-1^{+0}_{-0}	$8.42^{+0.20}_{-0.22}$	$0.21^{+0.04}_{-0.05}$	-1^{+0}_{-0}	$2455258.2^{+2.2}_{-0.9,4}$	-1^{+0}_{-0}	-1^{+0}_{-0}
Ross 128 HARPS	$2P_{\text{ecc}} + \text{GP-QP}$	$0.27^{+0.13}_{-0.14}$	$5.3^{+0.8}_{-0.8}$	$-0.85^{+0.06}_{-0.06,5}$	$0.0^{+0.3}_{-0.3}$	$2459106.80^{+0.94}_{-0.94}$	$0.80^{+0.14}_{-0.24}$	167^{+9}_{-13}
Ross 128 RedDots	$2P_{\text{ecc}} + \text{GP-QP}$	$0.50^{+0.14}_{-0.17}$	$4.64^{+0.13}_{-0.60}$	$-0.26^{+0.09}_{-0.17}$	$-0.05^{+0.13}_{-0.13}$	$2459104.9^{+0.24}_{-0.16}$	$0.12^{+0.24}_{-0.36}$	$166^{+10}_{-2.9}$
Ross 128 HARPS+Carmenes	$2P_{\text{ecc}} + \text{GP-QP}$	$0.25^{+0.14}_{-0.18}$	$5.8^{+0.60}_{-0.80}$	$0.57^{+0.28}_{-0.24}$	$-0.31^{+0.16}_{-0.18}$	$2459101.3^{+1.0}_{-2.0,9}$	$0.47^{+0.36}_{-0.19}$	$2.4^{+2.9}_{-1.9}$
GJ 832 HARPS	$2P_{\text{circ}} + \text{GP-QP}$	$0.5^{+0.6}_{-0.69}$	$358^{+0.80}_{-0.65}$	—	—	$2455599^{+2.09}_{-3.0,3}$	—	—
GJ 674 HARPS	$2P_{\text{circ}} + \text{GP-QP}$	$0.18^{+0.09}_{-0.09}$	$4.47^{+0.14}_{-0.13}$	—	—	$2455222.1^{+3.3}_{-3.8,3}$	—	—
Ross 128 HARPS	$2P_{\text{circ}} + \text{GP-QP}$	$0.37^{+0.11}_{-0.11}$	$3.12^{+0.43}_{-0.6,7}$	—	—	$2459102.58^{+3.23}_{-0.22}$	—	—
Ross 128 RedDots	$2P_{\text{circ}} + \text{GP-QP}$	$0.70^{+0.17}_{-0.22}$	$1.68^{+0.33}_{-0.38,41}$	—	—	$2459105.8^{+2.1}_{-0.19}$	—	—
Ross 128 HARPS+Carmenes	$2P_{\text{circ}} + \text{GP-QP}$	$0.453^{+0.009}_{-0.206}$	$4.0342^{+0.38,41}_{-0.0006}$	—	—	$2459104.10^{+0.19}_{-2.51}$	—	—

Table G.10. Bayesian posteriors for the parameters of planet 2 obtained during the model comparison.

		K_2	P_2	$\sqrt{e_2} \cos \omega_2$	$\sqrt{e_2} \sin \omega_2$	$t_{0,2}$	e_2	ω_2
GJ 832 HARPS	0P							
GJ 674 HARPS	0P							
Ross 128 HARPS	0P							
Ross 128 RedDots	0P							
Ross 128 HARPS+Carmenes	0P							
GJ 832 HARPS	1P ^{ecc}							
GJ 674 HARPS	1P ^{ecc}							
Ross 128 HARPS	1P ^{ecc}							
Ross 128 RedDots	1P ^{ecc}							
Ross 128 HARPS+Carmenes	1P ^{ecc}							
GJ 832 HARPS	1P ^{circ}							
GJ 674 HARPS	1P ^{circ}							
Ross 128 HARPS	1P ^{circ}							
Ross 128 RedDots	1P ^{circ}							
Ross 128 HARPS+Carmenes	1P ^{circ}							
GJ 832 HARPS	2P ^{ecc}	$18.0^{+0.9}$	3790^{+52}	$0.09^{+0.05}$	$0.06^{+0.12}$	2456318^{+44}	$0.025^{+0.014}$	62^{+3}
GJ 674 HARPS	2P ^{ecc}	$2.76^{+0.8}$	$36.709^{+0.012}$	$0.28^{+0.03}$	$0.41^{+0.16}$	$2457353.3^{+1.1}$	$0.27^{+0.089}$	55^{+38}
Ross 128 HARPS	2P ^{ecc}	$1.245^{+0.024}$	$9.8568^{+0.0009}$	$-0.371^{+0.015}$	$-0.309^{+0.013}$	$2459204.88^{+0.14}$	$0.233^{+0.089}$	$173.1^{+1.1}$
Ross 128 RedDots	2P ^{ecc}	$1.3^{+0.9}$	$11.0^{+1.2}$	$0.2^{+0.3}$	$-0.1^{+0.3}$	$2459212.4^{+0.5}$	$0.23^{+0.085}$	$35.6^{+2.0}$
Ross 128 HARPS+Carmenes	2P ^{ecc}	$1.053^{+0.018}$	$9.8528^{+0.0029}$	$-0.190^{+0.012}$	$0.885^{+0.007}$	$2459213.26^{+0.17}$	$0.820^{+0.015}$	$102.1^{+0.4}$
GJ 832 HARPS	2P ^{circ}	$17.40^{+0.22}$	3771^{+40}			2456345^{+17}		
GJ 674 HARPS	2P ^{circ}	$2.6^{+0.3}$	$36.726^{+0.014}$			$2457391.9^{+0.7}$		
Ross 128 HARPS	2P ^{circ}	$1.18^{+0.14}$	$9.8556^{+0.0016}$			$2459204.2^{+0.4}$		
Ross 128 RedDots	2P ^{circ}	$1.43^{+0.14}$	$9.83^{+0.0915}$			$2459204.2^{+0.3}$		
Ross 128 HARPS+Carmenes	2P ^{circ}	$1.26^{+0.05}$	$9.8551^{+0.0016}$			$2459204.29^{+0.34}$		
GJ 832 HARPS	0P + GP-SHO							
GJ 674 HARPS	0P + GP-SHO							
Ross 128 HARPS	0P + GP-SHO							
Ross 128 RedDots	0P + GP-SHO							
Ross 128 HARPS+Carmenes	0P + GP-SHO							
GJ 832 HARPS	0P + GP-dHO							
GJ 674 HARPS	0P + GP-dHO							
Ross 128 HARPS	0P + GP-dHO							
Ross 128 RedDots	0P + GP-dHO							
Ross 128 HARPS+Carmenes	0P + GP-dHO							
GJ 832 HARPS	0P + GP-QP							
GJ 674 HARPS	0P + GP-QP							
Ross 128 HARPS	0P + GP-QP							
Ross 128 RedDots	0P + GP-QP							
Ross 128 HARPS+Carmenes	0P + GP-QP							
GJ 832 HARPS	1P ^{ecc} + GP-SHO							
GJ 674 HARPS	1P ^{ecc} + GP-SHO							
Ross 128 HARPS	1P ^{ecc} + GP-SHO							

Table G.10. continued.

		K_2	P_2	$\sqrt{e_2} \cos \omega_2$	$\sqrt{e_2} \sin \omega_2$	$t_{0,2}$	e_2	ω_2
Ross 128 RedDots	IP _{ecc} + GP-SHO	—	—	—	—	—	—	—
Ross 128 HARPS+Carmenes	IP _{ecc} + GP-SHO	—	—	—	—	—	—	—
GJ 832 HARPS	IP _{circ} + GP-SHO	—	—	—	—	—	—	—
GJ 674 HARPS	IP _{circ} + GP-SHO	—	—	—	—	—	—	—
Ross 128 HARPS	IP _{circ} + GP-SHO	—	—	—	—	—	—	—
Ross 128 RedDots	IP _{circ} + GP-SHO	—	—	—	—	—	—	—
Ross 128 HARPS+Carmenes	IP _{circ} + GP-SHO	—	—	—	—	—	—	—
GJ 832 HARPS	IP _{ecc} + GP-dSHO	—	—	—	—	—	—	—
GJ 674 HARPS	IP _{ecc} + GP-dSHO	—	—	—	—	—	—	—
Ross 128 HARPS	IP _{ecc} + GP-dSHO	—	—	—	—	—	—	—
Ross 128 RedDots	IP _{ecc} + GP-dSHO	—	—	—	—	—	—	—
Ross 128 HARPS+Carmenes	IP _{ecc} + GP-dSHO	—	—	—	—	—	—	—
GJ 832 HARPS	IP _{circ} + GP-dSHO	—	—	—	—	—	—	—
GJ 674 HARPS	IP _{circ} + GP-dSHO	—	—	—	—	—	—	—
Ross 128 HARPS	IP _{circ} + GP-dSHO	—	—	—	—	—	—	—
Ross 128 RedDots	IP _{circ} + GP-dSHO	—	—	—	—	—	—	—
Ross 128 HARPS+Carmenes	IP _{circ} + GP-dSHO	—	—	—	—	—	—	—
GJ 832 HARPS	IP _{ecc} + GP-QP	—	—	—	—	—	—	—
GJ 674 HARPS	IP _{ecc} + GP-QP	—	—	—	—	—	—	—
Ross 128 HARPS	IP _{ecc} + GP-QP	—	—	—	—	—	—	—
Ross 128 RedDots	IP _{ecc} + GP-QP	—	—	—	—	—	—	—
Ross 128 HARPS+Carmenes	IP _{ecc} + GP-QP	—	—	—	—	—	—	—
GJ 832 HARPS	IP _{circ} + GP-QP	—	—	—	—	—	—	—
GJ 674 HARPS	IP _{circ} + GP-QP	—	—	—	—	—	—	—
Ross 128 HARPS	IP _{circ} + GP-QP	—	—	—	—	—	—	—
Ross 128 RedDots	IP _{circ} + GP-QP	—	—	—	—	—	—	—
Ross 128 HARPS+Carmenes	IP _{circ} + GP-QP	—	—	—	—	—	—	—
GJ 832 HARPS	2P _{ecc} + GP-SHO	17.4 ^{+0.5}	3754 ⁺⁵⁸	0.14 ^{+0.08}	-0.00 ^{+0.10}	2456310 ⁺⁵³	0.030 ^{+0.027}	29 ⁺⁵⁰
GJ 674 HARPS	2P _{ecc} + GP-SHO	1.3 ^{+0.5}	63.5 ⁺⁵⁶	-0.00 ^{+0.08}	0.14 ^{+0.05}	2457349 ⁺³	0.030 ^{+0.022}	92 ⁺⁴⁷
Ross 128 HARPS	2P _{ecc} + GP-SHO	1.11 ^{+0.08}	9.8546 ^{+0.0015}	-0.00 ^{+0.12}	0.14 ^{+0.06}	2459203.20 ^{+0.25}	0.30 ^{+0.08}	15 ⁺⁶
Ross 128 RedDots	2P _{ecc} + GP-SHO	1.38 ^{+0.24}	9.89 ^{+0.13}	0.52 ^{+0.06}	0.14 ^{+0.06}	2459213.1 ^{+0.23}	0.14 ^{+0.08}	63 ⁺⁵⁶
Ross 128 HARPS+Carmenes	2P _{ecc} + GP-SHO	1.0 ^{+0.38}	9.8559 ^{+0.0017}	0.17 ^{+0.21}	0.0 ^{+0.3}	2459213.5 ^{+0.9}	0.14 ^{+0.12}	43 ⁺⁵⁹
GJ 832 HARPS	2P _{circ} + GP-SHO	17.5 ^{+0.5}	3751 ⁺⁵⁸	0.34 ^{+0.16}	-0.03 ^{+0.29}	2456351 ⁺²⁹	0.17 ^{+0.09}	43 ⁺³⁰
GJ 674 HARPS	2P _{circ} + GP-SHO	2.3 ^{+0.4}	36.730 ^{+0.023}	—	—	2457318.8 ^{+1.1}	—	—
Ross 128 HARPS	2P _{circ} + GP-SHO	1.34 ^{+0.22}	9.8560 ^{+0.0071}	—	—	2459213.97 ^{+0.36}	—	—
Ross 128 RedDots	2P _{circ} + GP-SHO	1.0 ^{+0.18}	9.88 ^{+5.6}	—	—	2459213.73 ^{+0.98}	—	—
Ross 128 HARPS+Carmenes	2P _{circ} + GP-SHO	1.54 ^{+0.04}	9.8538 ^{+0.0023}	—	—	2459213.95 ^{+0.23}	—	—
GJ 832 HARPS	2P _{ecc} + GP-dSHO	16.8 ^{+0.9}	3813 ⁺³⁰	0.05 ^{+0.09}	-0.17 ^{+0.11}	2456340 ⁺⁷⁷	0.05 ^{+0.03}	36 ⁺¹⁰⁶
GJ 674 HARPS	2P _{ecc} + GP-dSHO	-1 ⁺⁰	11.7 ^{+6.2}	-1 ^{+0.20}	-1 ⁺⁰	2459210 ⁺⁴	-1 ⁺⁰	-1 ⁺⁰
Ross 128 HARPS	2P _{ecc} + GP-dSHO	0.6 ^{+0.5}	9.83 ^{+0.18}	0.32 ^{+0.19}	0.2 ^{+0.3}	2459213.5 ^{+0.3}	0.28 ^{+0.22}	30 ⁺⁶²
Ross 128 RedDots	2P _{ecc} + GP-dSHO	1.47 ^{+0.15}	9.83 ^{+0.06}	0.28 ^{+0.17}	0.08 ^{+0.25}	2459213.5 ^{+0.4}	0.16 ^{+0.06}	35 ⁺²⁷
Ross 128 HARPS+Carmenes	2P _{ecc} + GP-dSHO	-1 ⁺⁰	-1 ⁺⁰	-1 ^{+0.13}	-1 ⁺⁰	2456351 ⁺²⁸	-1 ⁺⁰	-1 ⁺⁰
GJ 832 HARPS	2P _{circ} + GP-dSHO	17.5 ^{+0.4}	3761 ⁺⁵²	-1 ⁺⁰	-1 ⁺⁰	2456351 ⁺³³	-1 ⁺⁰	-1 ⁺⁰

Table G.10. continued.

		K_2	P_2	$\sqrt{e_2} \cos \omega_2$	$\sqrt{e_2} \sin \omega_2$	$t_{0,2}$	e_2	ω_2
GJ 674 HARPS	2P _{circ} + GP-dSHO	$0.9^{+0.4}_{-0.65}$	78^{+10}_{-41}	—	—	2457320^{+49}_{-10}	—	—
Ross 128 HARPS	2P _{circ} + GP-dSHO	$0.97^{+0.05}_{-0.12}$	$9.8558^{+0.0015}_{-0.0015}$	—	—	$2459213.92^{+0.29}_{-0.23}$	—	—
Ross 128 RedDots	2P _{circ} + GP-dSHO	$1.27^{+0.12}_{-0.08}$	$9.78^{+0.08}_{-0.08}$	—	—	$2459204.5^{+0.7}_{-0.43}$	—	—
Ross 128 HARPS+Carmenes	2P _{circ} + GP-dSHO	$0.868^{+0.036}_{-0.016}$	$9.8525^{+0.0014}_{-0.0019}$	—	—	$2459203.35^{+0.53}_{-0.16}$	—	—
GJ 832 HARPS	2P _{ecc} + GP-QP	$17.5^{+0.5}_{-0.5}$	3761^{+60}_{-75}	$0.10^{+0.09}_{-0.12}$	$-0.03^{+0.12}_{-0.11}$	2456327^{+48}_{-57}	$0.027^{+0.026}_{-0.019}$	37^{+60}_{-56}
GJ 674 HARPS	2P _{ecc} + GP-QP	—	—	—	—	—	—	—
Ross 128 HARPS	2P _{ecc} + GP-QP	$1.45^{+0.11}_{-0.13}$	$9.8547^{+0.0011}_{-0.0011}$	$0.51^{+0.06}_{-0.08}$	$0.31^{+0.09}_{-0.10}$	$2459203.29^{+0.24}_{-0.21}$	$0.36^{+0.07}_{-0.08}$	31^{+9}_{-9}
Ross 128 RedDots	2P _{ecc} + GP-QP	$1.10^{+0.12}_{-0.11}$	$9.88^{+0.08}_{-0.08}$	$-0.16^{+0.17}_{-0.11}$	$-0.22^{+0.06}_{-0.10}$	$2459204.0^{+0.5}_{-0.51}$	$0.10^{+0.08}_{-0.08}$	72^{+9}_{-61}
Ross 128 HARPS+Carmenes	2P _{ecc} + GP-QP	$1.21^{+0.12}_{-0.12}$	$9.8551^{+0.0011}_{-0.0010}$	$0.13^{+0.11}_{-0.11}$	$-0.25^{+0.10}_{-0.09}$	$2459213.81^{+0.21}_{-0.22}$	$0.09^{+0.06}_{-0.04}$	5^{+1}_{-4}
GJ 832 HARPS	2P _{circ} + GP-QP	$17.5^{+0.5}_{-0.4}$	3747^{+21}_{-21}	—	—	2456349^{+34}_{-34}	—	—
GJ 674 HARPS	2P _{circ} + GP-QP	$1.58^{+0.04}_{-0.07}$	$36.184^{+0.017}_{-0.017}$	—	—	$2457378.53^{+0.72}_{-0.90}$	—	—
Ross 128 HARPS	2P _{circ} + GP-QP	$0.72^{+0.25}_{-0.38}$	$10.13^{+0.05}_{-0.05}$	—	—	$2459211.7^{+2.2}_{-2.2}$	—	—
Ross 128 RedDots	2P _{circ} + GP-QP	$1.00^{+0.38}_{-0.18}$	$9.89^{+0.057}_{-0.15}$	—	—	$2459213.5^{+0.8}_{-0.3}$	—	—
Ross 128 HARPS+Carmenes	2P _{circ} + GP-QP	$1.258^{+0.127}_{-0.006}$	$9.85611^{+0.00009}_{-0.00094}$	—	—	$2459204.15^{+0.03}_{-0.08}$	—	—